Challenge Journal of
CONCRETE RESEARCH LETTERS

Vol.12 No.1 (2021)

absorption acoustic emission artificial neural network compressive strength concrete corrosion cracking ductility durability energy absorption ferrocement flaky aggregate fly ash fracture mechanical properties mortar reinforced concrete self-compacting concrete silica fume strengthening superplasticizer tensile strength waste disposal water absorption w ility

ISSN 2548-0928

TULPAR
ACADEMIC PUBLISHING

Challenge Journal of Concrete Research Letters

E-mail: *cjcrl@challengejournal.com*

Web page: *cjcrl.challengejournal.com*

TULPAR Academic Publishing
www.tulparpublishing.com

Challenge Journal of Concrete Research Letters

CONTENTS

Research Articles

TULPAR ACADEMIC PUBLISHING

Challenge Journal of Concrete Research Letters

Research Article

Effect of high temperature on SCC containing fly ash

Mehmet Canbaz [a,*], Erman Acay [a]

[a] *Department of Civil Engineering, Eskişehir Osmangazi University, 26480 Eskişehir, Turkey*

ABSTRACT

The effect of high temperature on self-compacting concrete, which contains different amounts of fly ash, has been investigated. By considering the effect of concrete age and increased temperatures, the optimum fly ash-cement ratio for the optimum concrete strength is determined using experimental studies. Self-compacting concrete specimens are produced, with fly ash/cement ratios of 0%, 20% and 40%. Specimens were cured for 28, 56 and 90 days. After curing was completed, the specimens were subjected to temperatures of 20°C, 100°C, 400°C, 700°C and 900°C for three hours. After the cooling process, tests were performed to determine the unit weight, ultrasonic pulse velocity and compressive strength of the specimens. According to the experiment results, an increase in fly ash ratio causes a decrease in the compressive strength of self-compacting concrete. However, it positively contributes to self-compaction and strength loss at high temperatures. The utilization of fly ash in concrete significantly contributes to the environment and the economy. For this reason, the addition of 20% fly ash to concrete is considered to be effective.

ARTICLE INFO

Article history:
Received 2 June 2020
Revised 21 August 2020
Accepted 10 September 2020

Keywords:
Self-compacting concrete
Fly ash
High temperature
Concrete age

1. Introduction

Reinforced high-performance concrete with chemical admixtures and mineral additives has been employed in modern structures. The behaviour of this concrete at high temperatures should be well understood. Due to the low porosity of concrete, this concrete is a denser structure with a high-temperature performance that is lower than the high-temperature performance of normal strength concrete (Scherefler et al., 2003). In the class of high-performance concrete, self-compacting concrete is another type of concrete. Self-compacting concrete (SCC), which is defined as concrete without the use of internal or external vibration and compacting, is self-placed in a mold (Leemann et al., 2006; Kamal et al., 2017). The two basic features of SCC are the use of large amounts of fine materials and the use of a new-generation superplasticizer, which provide high fluidity and segregation resistance. As a viscosity-enhancing material in SCC, a mineral additive may be employed (Felekoğlu et al., 2007; Apeh, 2019; Agwa and Ibrahim, 2019). One of the most important additives is fly ash (FA). FA decreases bleeding by reducing the rate of hydration. It improves the workability of concrete due to spherical particles and provides a stable structure due to the increased amount of fine material in the concrete. Studies of SCC generally include an investigation of the properties of fresh and hardened SCC. Currently, significant experience and the development of SCC have been achieved. However, some problems remain unsolved, such as the behavior of SCC at high temperatures (Altın, et al., 2006). The effect of high temperature on concrete is dependent on the temperature, test period, structure of the cement paste phase, and aggregate type. These changes cause a significant decrease in the compressive strength of concrete (Akman, 2000). The relationship between the porosity of concrete and the compressive strength of concrete is known. The compressive strength of concrete increases as the porosity of concrete decreases (Vodak et al., 2006). When cement paste and aggregate are exposed to high temperatures, physical and chemical degradation causes changes in the distribution of the total porosity and pore size. Generally, hardened cement paste expands at temperatures from 20-200°C. Due to the effect of different densities, concrete shrinks and an expansion in the aggregates is

* *Corresponding author*. Tel.: +90-222-239-3750 ; Fax: +90-222-239-3613 ; E-mail address: mcanbaz@ogu.edu.tr (M. Canbaz)
ISSN: 2548-0928 / DOI: https://doi.org/10.20528/cjcrl.2021.01.001

observed at temperatures above 200°C. These changes cause an increase in pore size (Alonzo et al., 2003). Up to 500°C, water from the capillary and the gel water is removed, which causes a significant increase in the total void volume (Haddad and Shannis, 2004). The total pore volume increases to 600°C. This increase is higher than the expected total pore volume, which reveals weight loss similarities in concrete. This finding may be attributed to the increase in voids due to deterioration of the solid phase or formed micro cracks. The micro pore ratio is reduced at high temperatures, which may cause sintering at temperatures above 900°C (Alonzo et al., 2003). Factors such as free water migration and evaporation, the loss of bound and absorbed water at 450°C, calcium hydroxide decomposition, as quartz constitutes the majority of sand at 575°C, the transition of α-quartz to β-quartz occurs, and a deterioration in the structure of calcium silicate hydrate (CSH) at 400-600°C serve an important role in the strength loss of concrete that is exposed at high temperatures (Felicetti and Gambarova, 1998). Three different phases of water are observed in concrete: adsorption water, which connects the solid element of CSH in cement gel paste; the chemically bound water in hydrate; and water that is free in the capillary pores. During the production of concrete, which is dependent on the cement type and water/cement ratio, free water that is available to 4% of the volume of the concrete vaporizes at 100°C and chemically bonded water vaporizes at 300°C. Due to the effect of temperature, shrinkage that occurred after water loss and high vapor pressure caused cracking and spalling of the concrete covering of the reinforcement concrete in this stage. Due to the destruction of the concrete covering, a reinforcement concrete steel bar comes into contact with hot gas at the beginning of the fire (Akman, 2000). During placement, concrete is a wet and porous material. Normal- and high-strength concretes at 70°C retain a maximum of 99% of the initial mass. Between 70-120°C, the free water in the concrete evaporates. At 120°C, normal- and high-strength concrete lose the same amount of water. The loss of mass is approximately 1.4%. The largest amount of weight loss, which is approximately 7%, occurs from 120 to 300°C due to the drying of the bound water in the hardened concrete. The loss of mass between 300 and 600°C is less important due to the small amount of calcium hydroxide in high-strength concrete and the result of pozzolanic effect of the mineral additive (Cülfik, 2001). The length of exposure to temperature, humidity conditions, heating and cooling rates and loading conditions are contributing factors to the compressive strength of the concrete that is exposed to high temperatures (Neville, 2000). In normal-strength concrete, the uniaxial compressive strength at high temperatures in the first stages causes an increase in the compressive strength with an increase in temperature. The strength at temperatures above 200°C begins to decrease. The compressive strength at 700°C decreases by 80% compared with the initial value (Cülfik, 2001). In the first phase, the increase in strength of the concrete produced with siliceous aggregates is significant as the strength of the adherence between the cement and the aggregate is substantial in silica aggregates (Savva et al., 2005). Significant reductions in tensile strength are obtained by the splitting concrete test at temperatures from 100°C, and maximum losses of 70% are attained at 600°C (Guise et al., 1996). With different types and amounts of pozzolan in concrete, a continuous decrease in the modulus of elasticity with temperature has been observed (Savva et al., 2005). The addition of FA and high temperatures caused a significant decrease in the modulus of elasticity was observed (Papayianni and Valliasis, 2005).

Few studies have addressed the effect of high temperatures on SCC (Jin and Yong, 2006; Heiza, 2012; Mathews et al., 2020). When considering the strength performance of SCC, they are located in the class of high-strength concrete (HSC). Thus, the behavior of SCC at high temperatures can be evaluated by the performance of HSC at high temperatures. Compared with normal concrete, HSC at high temperatures is considered to be less durable. The amount of pore reduction in concrete is dependent on the type of aggregate; due to the evaporation of water in cement gel, internal pressure occurs. Concrete expands at high temperatures due to a polymorphic conversion in aggregates and changes in the concrete thermal expansion coefficient. Due to the high moisture content, concrete becomes fractured (Ye et al., 2007). For this reason, HSC that contains fewer pores at high temperatures can incur a greater amount of damage. This situation also applies to SCC. To minimize damage that will occur in HSC and SCC at high temperatures, the use of polypropylene fibers that melt at high temperatures is proposed to form pores in the concrete (ERMCO, 2005). To increase the resistance of HSC to high temperatures, the recommended method is the use the lightweight aggregate. High temperatures are considered to affect the mineralogical structure (Helal and Heiza, 2006). The material properties of HSC with the effect of temperature differ from the material properties of normal-strength concrete; these differences were reported to be more prominent between 25 and 400°C. In this range, high-strength concrete showed a strength loss that was more rapid than the strength loss in normal strength concrete (Phan and Carino, 1998). HSC that contains silica fume was determined to be explosively fragmented (Lawson et al., 2000). The relative residual strength is significant (Poon et al., 2001). The strength of SCC increased at temperatures 150-300°C. The loss of the mechanical properties of SCC increased at temperatures above 300°C due to the formation of permanent strain and micro cracks (Hana et al., 2009). The coefficient of thermal expansion of SCC were determined to be higher than the coefficient of thermal expansion of normal concrete at high temperatures. The use of lightweight aggregate in SCC reduces the coefficient of thermal expansion (Topçu and Uygunoğlu, 2009). Currently, the use of SCC is common. An increasing number of studies are underway to improve the properties of fresh and hardened SCC. This study aimed to improve the properties of fresh SCC by replacing cement with 20-40% FA (Acay, 2010). In addition, the effect of elevated temperatures on the durability properties of SCC, which has been insufficiently explored, was also investigated. Compared to conventional concrete, higher cement and lower water

rates are used in SCC production. Therefore, the strength of SCC can be high. High strength concretes can spall under the effect of high temperature due to the water vapor pressure in the internal structure. Here, by using less cement with the use of FA, it is aimed not only to increase the workability, but to reduce the damage under high temperature effect with decreasing rigidity.

2. Experimental Study

2.1. Materials

Cement: Type R CEM I 42.5 cement was employed in the experiment. The chemical properties of this cement are listed in Table 1.

Fly Ash (FA): The entire experimental study was performed using F-type FA from the Tunçbilek Company. The physical and chemical properties of the FA are listed in Table 2.

Superplasticizer: Glenium C303 superplasticizer produced by the YKS Company was employed. The properties of the new-generation superplasticizer are listed in Table 3.

Water: Eskişehir tap water was employed. The chemical analysis of the drinkable water is provided in Table 4.

Aggregate: In this study, crushed sand and crushed stones, which were obtained from Çimsa Ready Mixed Concrete, were employed. The granulometry of the aggregate mixture is presented in Fig. 1, and the properties of the aggregates are listed in Table 5.

Table 1. Properties of the cement.

SiO_2	CaO	Al_2O_3	Fe_2O_3	MgO	Na_2O+0.66 K_2O	SO_3	Cl^-
19.4	63.78	5.2	2.38	1.85	0.62	2.84	0.009

Table 2. Properties of the fly ash.

Spec. Gravity	Free CaO	>45μm, %	Reactive CaO	Activite indeks	SO_3	Cl^-	LOI
2.28	0.06	26.2	2.63	82.6	0.41	0.0088	0.56

Table 3. Properties of the superplasticizer.

Cl^-, %	Chemical Structure	Alkali, %	Color	Density, kg/dm³
0.1	Polycarbocsilic Ester-based liquid	3	Light green	1.02-1.06

Table 4. Chemical analysis of the water (mg/lt).

pH	Na_2O	Ka_2O	Cl^-	SO_4	Zn	Pb	P_2O_3	NO_3	∑alkalinity	Color
7.8	52	11	66	23	10	0.05	1.5	0.1	8	Crystal clear

Table 5. Properties of the aggregate.

Size mm	Fineness modulus	Filler content %	Water absorption %	Saturated density kg/dm³
0-7	2.46	6	1.59	2.63
7-15	6.01	0.9	0.62	2.67
15-22	6.96	0.4	0.42	2.70

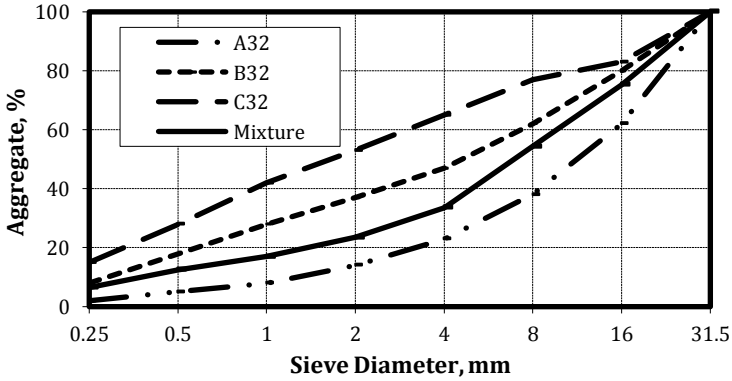

Fig. 1. Granulometry of aggregate mixture.

2.2. Method and tests

In this study, three different series, depending on the rate of FA, were determined at the end of the trial mix designs to fulfil the requirements of SCC. The mixing ratios of these series are shown in Table 6. 15×15×15 cm^3 cubic specimens of each mixture were prepared. In this study, it is aimed to increase the fine material ratio for self-compressibility. Therefore, FA was not added to the mixture instead of cement as in other studies (Mohammed et al., 2014; Topçu and Uygunoğlu, 2009). Slump-flow test to determine the filling ability, L-box test to determine the passing ability and sieve segregation test to determine the segregation resistance of SCC were conducted on fresh SCC. Concrete specimens were cured in standard conditions until 28-day, 56-day and 90-day strengths were attained. The specimens were exposed to temperatures of 20°C, 100°C, 400°C, 600°C, and 900°C for three hours according to TS EN 1363-1. The heating rate was 6°C/min. The specimens were slowly cooled to six hours in ambient air. Unit weight, ultrasonic pulse velocity, and compressive strength tests were performed. The effect of high temperature on the reduction in unit weight, the ultrasonic pulse velocity (UPV), and the compressive strength was investigated.

Table 6. Mixing ratio, kg/m^3.

	FA-0	FA-20	FA-40
Cement	450	450	450
Fly Ash	0	90	180
Water	175	175	175
Fine Aggregate (0-7)	992	931	870
Coarse Aggregate (7-15)	430	404	377
Coarse Aggregate (15-22)	313	294	275
Admixture	4	4	4

3. Discussion

3.1. Properties of fresh SCC

The flow diameter and the average time to attain T50 cm of the SCC series by adding different amounts of FA are shown in Fig. 2. The ratio of FA was observed to increase with an increase in diameter of the flow. The increase in the flow diameter can enhance the workability of the SCC by FA. The time to attain T50 cm of SCC flow decreased with an increase in the ratio of FA. FA causes a lubrication effect in SCC due to its round-grained shape and increases the rate of flow of SCC. If a slump-flow test, which is a common method for determining the filling ability of SCC, is considered, the flow diameter of SCC should fall within 650 to 800 mm for acceptable filling ability. According to the Europe Ready Mixed Concrete Association's (ERMCO) flow diameter classification, all mixtures are in the SF2 group. For the time to attain T50, all mixtures are in the VS2 group because all T50 values exceed 2 seconds. The increase in the amount of fine material and the round shape of FA positively affected the filling ability of SCC.

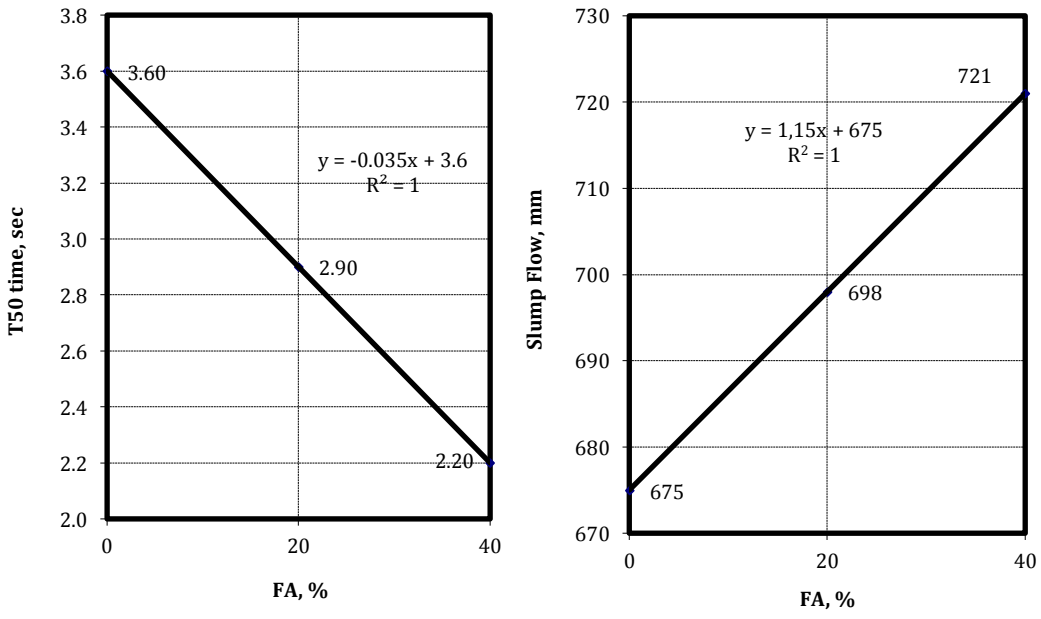

Fig. 2. Slump-flow test results of SCC.

To measure the passing ability of SCC, the most common test is the L box test; the results are provided in Fig. 3. The ratio of FA, which is measured by SCC's ability to pass between reinforcement bars, increased. Due to the lubrication effect of FA, a reduction in the wall effect is considered. As shown in Fig. 4, the proportion with regards to height level increases the proportion of FA and an increase in the passing rate to 0.91. This increase can be explained by an increase in the amount of fine particles in the mixture. According to the classification of the ERMCO passing rate, all types of mixtures are in the PA2 group as all values exceed 0.8. With the increase in FA amount, the decrease of coarse grains in the mixture and the round shape of FA positively affected the passing ability of SCC.

Sieve segregation test results of SCC are shown in Fig. 4. Segregation decreased with the use of FA in the SCC mixtures. The reason for this decrease can be attributed to the increase in the amount of binding. It can be used in inert mineral additives in SCC, but in this case the segregation resistance may decrease. However, since FA is a pozzolanic material, the segregation resistance of SCC is positively affected by the increase in cohesion in the internal structure.

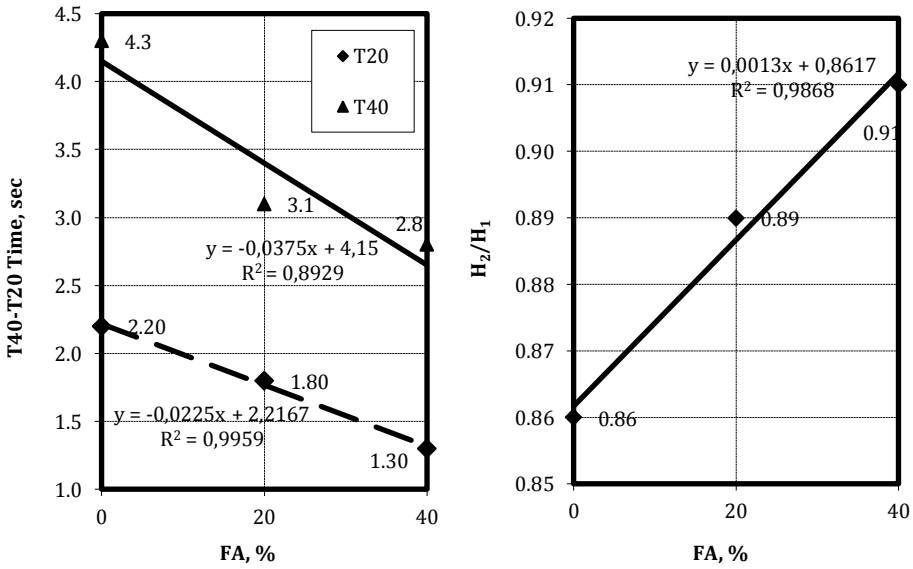

Fig. 3. L box test results of SCC.

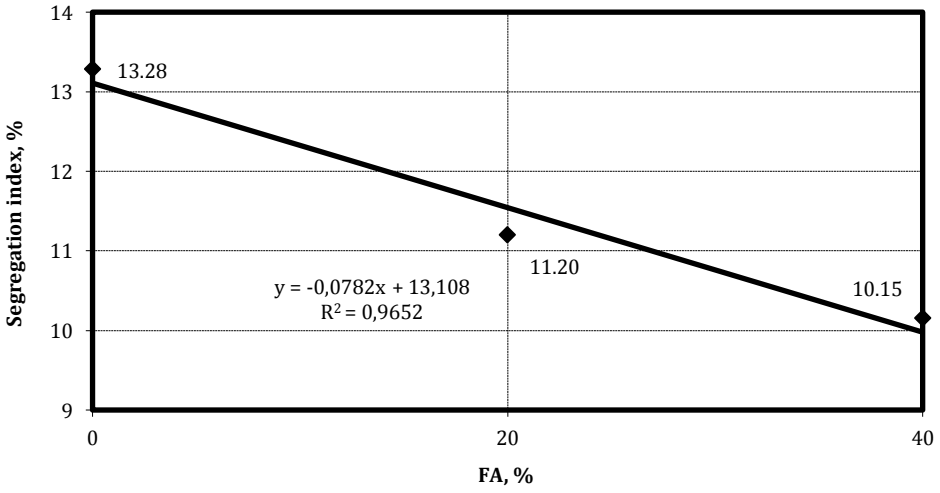

Fig. 4. Sieve segregation test results of SCC.

The lubrication effect of FA is significant in terms of workability. Grains in the form of small spheres, as shown in Fig. 5, simplify self-placing and compaction. Calcium silicate hydrates the structures that formed by reaction of FA with calcium hydroxide at the end of the cement hydration reactions, improves strength and increases compactness. Thus, the increase in compactness decreases segregation.

3.2. Properties of hardened SCC

The unit weight of SCC specimens at different ages are provided in Fig. 6. The unit weight of the specimens with 40% FA at 28 days decreased by 1.8%. The unit weight of the control specimens at 56 days was 2.4 kg/dm^3. With the addition of 20% FA, the unit weight of the mixture decreased by 0.7%; with 40% FA, the unit weight

decreased by 1.4%. The unit weight of the 90-day control specimens was 2.42 kg/dm^3. With 20% FA, the unit weight decreased by 1.3%; with 40% FA, the unit weight decreased by 2.6%. The largest reduction in the 90-day specimens that contain 40% FA was observed. As the specific gravity of FA is less than the specific gravity of the aggregate weight, a decrease in the unit weight was observed. Ninety days of FA reaction produces a low specific weight; as a result, the decreasing rate of the unit weight increases.

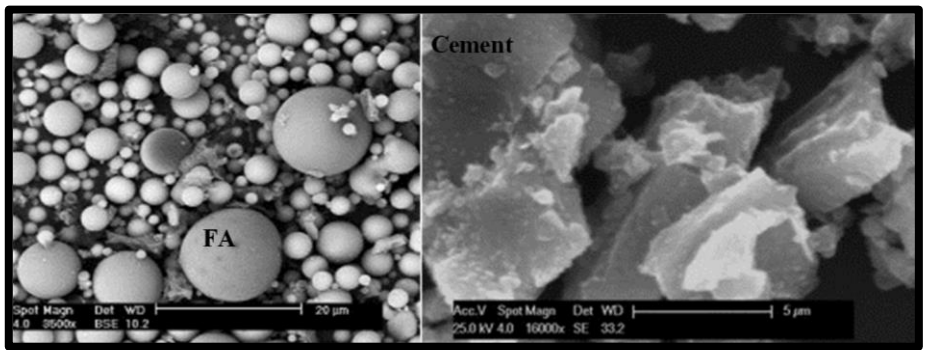

Fig. 5. Shape effect of cement and FA particles (Mohammed et al., 2014; Patrick et al., 2011).

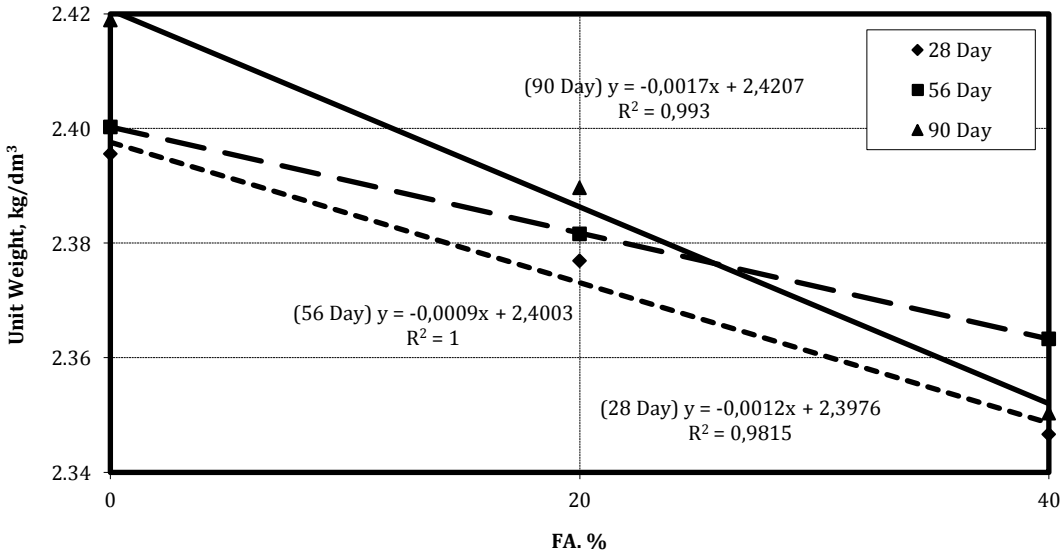

Fig. 6. Unit weight of SCC.

The results for UPV are shown in Fig. 7. In the experiments, the pulse velocity of the 28-day and 56-day control mixtures were determined. An increase of 20% FA produced an increase in velocity; 40% FA caused a decrease in velocity. These results indicate that the use of 20% FA to reduce the pores within the hardened concrete, causes an increase in the UPV. In the case of a higher rate of usage of FA, a reduction in the amount of coarse aggregate produced a decrease in the UPV. FA caused a reduction in coarse aggregate and the UPV, which is more apparent after 90 days. The pulse velocity of the concrete increases with an increase in age and the highest velocity rate values were determined on day 90.

Depending on the unit weight and the UPV test results, the dynamic elasticity modulus values were calculated, as shown in Fig. 8. The dynamic modulus of elasticity after 28 and 56 days using a 20% increase in FA produced an increase, whereas a mixture of 40% FA produced a decrease. For 90 day specimens, the modulus of elasticity linearly decreased with the use of FA. The decrease in UPV with the increase of FA on the 90th day can be explained as the less volume coating of the products that occur with the increase of pozzolanic reactions and the decrease of coarse aggregate.

The compressive strength test results at different ages are shown in Fig. 9. In the experiments conducted after 28 days and 90 days, the compressive strength decreased with the addition of FA. The 56-day compressive strength increased with 20% FA but decreased with 40% FA. The compressive strength of concrete increases with age, and the highest values were measured in the experiments that were conducted after 90 days. Studies have shown that the effect of ash on concrete compressive strength occurs after 56 days (Güçlüer, and Ünal, 2010). In this study, it was seen that the strength of the control concrete could not be obtained up to 90 days. Water and plasticizer remained the same despite the addition of ash. In this case, the necessary environment for the reaction of the ash with cement hydration products was not sufficiently formed. Therefore, the expected strength increase did not occur.

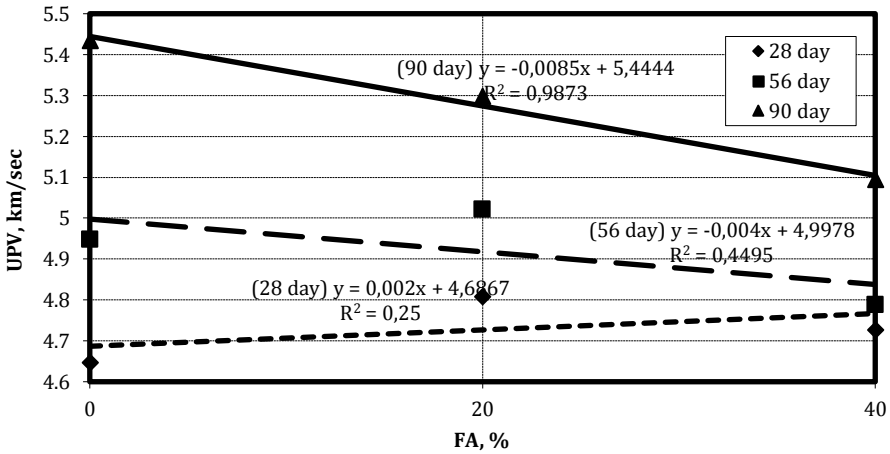

Fig. 7. UPV of SCC.

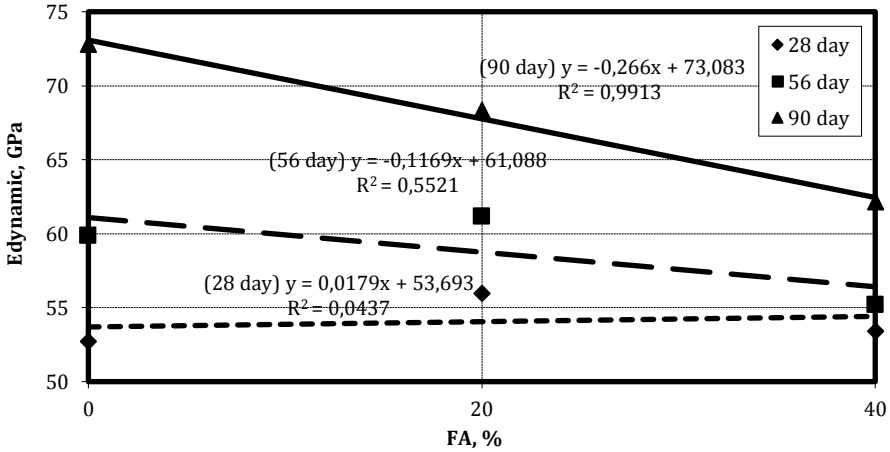

Fig. 8. Dynamic modulus of elasticity of SCC.

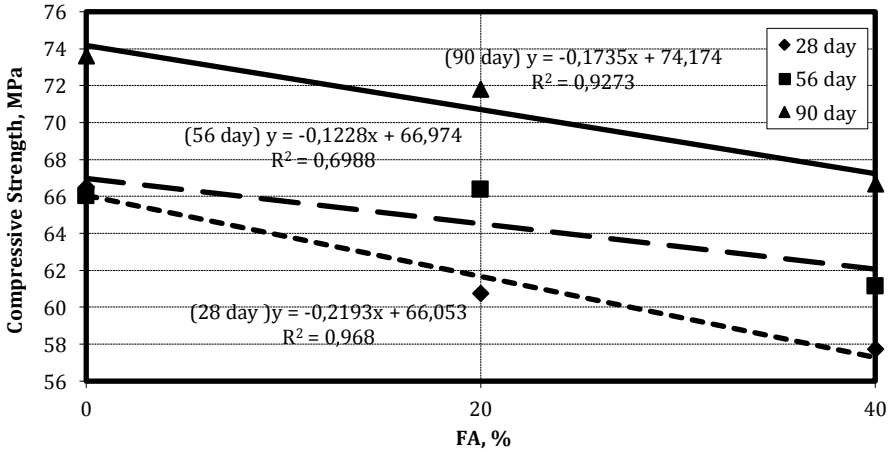

Fig. 9. Strength of SCC.

3.3. Properties of SCC subjected to high temperatures

The SCC specimens that were subjected to standard curing conditions for 28 days were exposed to temperatures of 100, 400, 700 and 900°C for three hours. The unit weight loss caused by the high temperature effect were calculated, as shown in Fig. 10. The effect of high temperatures to 700°C on the unit weight loss is approximately 5%, whereas the unit weight loss at 900°C increased above 10%. When the temperature increased above 100°C, the free water in the apparent pores evaporates, which causes the unit weight to suddenly decrease. The water in the remaining pores in the concrete evaporate at a slower rate, which causes unit weight reduction at a slower rate to 700°C. At temperatures above 700°C the unit weight rapidly declines with the restructure of CSH and limestone aggregates, which turn into lime. With the addition of FA and an increase in temperature, the

unit weight loss increased. A maximum unit weight loss of 14% was attained at 900°C as a high proportion of FA is employed. As a result, a reduction in the aggregates is observed due to the expansion effect of high temperatures on the chemical structure binding phase, which facilitates the deterioration of the unit weight. The unit weight loss for the 56-day SCC control specimens increased above 15% when exposed to a maximum temperature of 900°C. The unit weight loss of the 56-day specimens suddenly increased with an increase in temperature to 200°C and above 700°C. No significant change in unit weight wffas observed between 200-700°C. A reduction in unit weight loss occurred with the addition of a higher amount of FA in SCC at high temperatures. The unit weight loss decreased as a result of filling pores and became a stronger structure with products due to the reaction between FA and calcium hydroxide after 56-days. As the temperature increases, the sudden unit weight losses for 90-day specimens decreased and a more linear reduction is observed. An increase in temperature and the addition of FA generates a unit weight loss behaviour that is similar to the control specimens. After 90 days, the reaction of the FA and cement hydration products are predominantly complete; as a result, the variation in unit weight loss is reduced. As shown in Fig. 10, when we examine the increased percentage of FA with high temperature, an increase in the unit weight loss and concrete age is observed. The unit weight losses with 0%, 20% and 40% FA added to the specimens at high temperatures are similar.

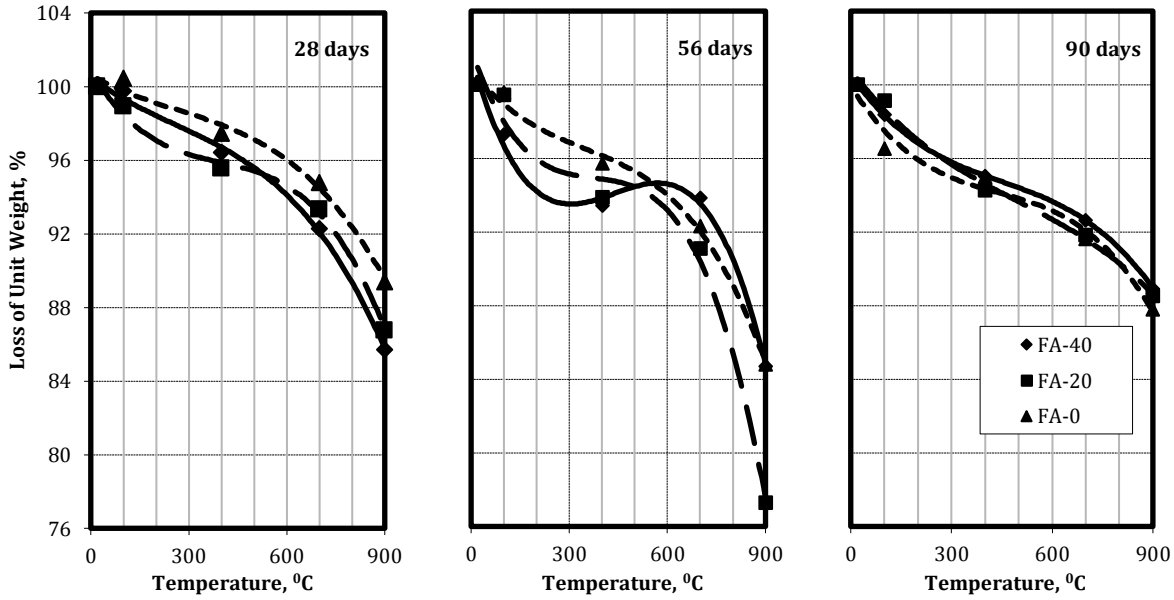

Fig. 10. Relative unit weight according to the temperature of SCC.

UPV loss for SCC specimens that were exposed to high temperature are shown in Fig. 11. The UPV loss of the control specimens for a maximum temperature of 900°C is less than 50%. With increasing temperature, the UPV decreased, whereas this reduction showed variable behaviour after the addition of FA to SCC above 700°C. The UPV losses decrease in the control concrete as the temperature increases. If high proportions of FA are added, the UPV decreases to 80%. At 28 days, the levels of reaction between FA and the products of hydration of cement are considered to be lower. When cured for 56 days and subjected to high temperatures during the UPV experiments, the specimens with FA showed the best results at temperatures between 400°C and 700°C. At 56 days, the reaction between FA and cement hydration products accelerates and reduce the pores, which reduce UPV losses. The restructure of the resulting products at high temperatures is considered to cause an increase in losses in UPV. At a curing time of 90 days, UPV losses are reduced by an average of 60% at 900°C. The UPV of 90 day specimens with a temperature increase reveals a linear increase in losses. By FA addition, the variation in losses are reduced at high temperatures. The addition of FA to 90 day specimens had a positive effect on UPV loss. FA reaction products increase the compaction of concrete; its effect on the pulse velocity loss rate is considered to be positive.

A loss of dynamic modulus of elasticity for the specimens that were exposed to different temperatures are shown in Fig. 12. The control specimens that were exposed to temperature increases to 900°C experience an accelerated loss of dynamic modulus of elasticity, which exceeded 72%. A dynamic modulus of elasticity loss for 28-day specimens showed a linear increase with an increase in temperature with the addition of FA. FA is considered not to completely react at an early age, which increases the loss of the dynamic elasticity modulus. At the curing time of 56 days, the loss of dynamic modulus of elasticity showed variable behaviour with the addition of FA in SCC. The dynamic modulus of elasticity of the control specimens decreased to 700°C. Considering the dynamic modulus of elasticity, a significant decrease was observed. At a maximum temperature of 700°C, a slower loss in the dynamic modulus of elasticity occurs for specimens with the addition of 40% FA compared with the addition of 20% FA as the hydration of cement continued

in concrete and its products react to the high ratio of FA. The dynamic modulus of elasticity loss of 90-day specimens with FA positively affected compared with the control specimen with temperature increases. Losses in the dynamic modulus of elasticity obtained more positive results due to FA increases compactness of binding paste and strengthening of the structure by the reaction products.

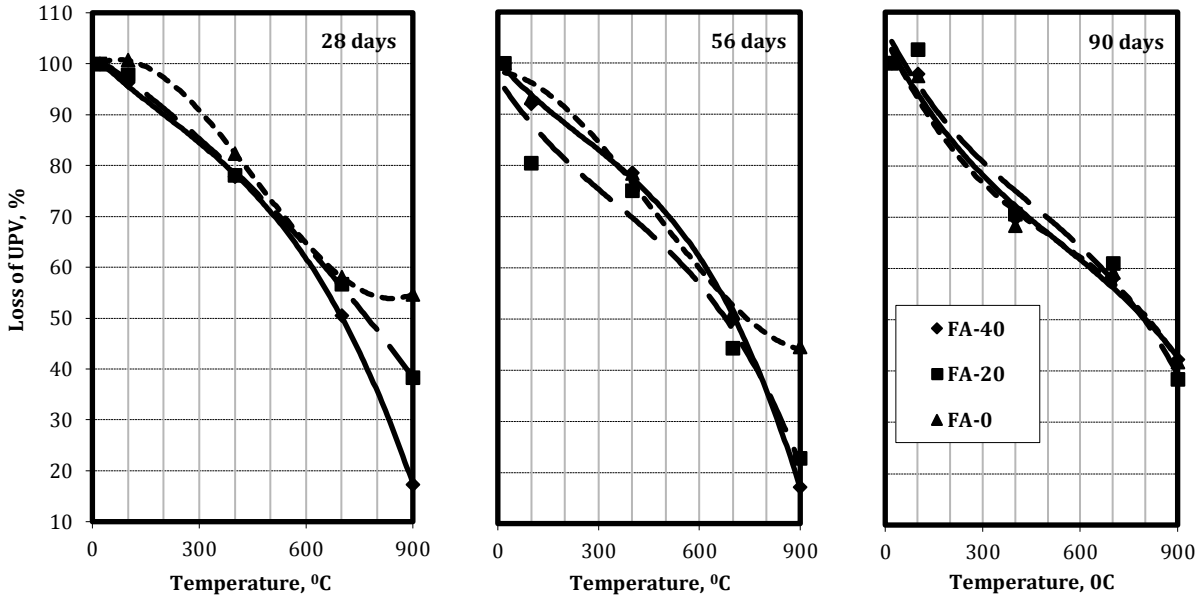

Fig. 11. Relative UPV values of SCC according to the temperature.

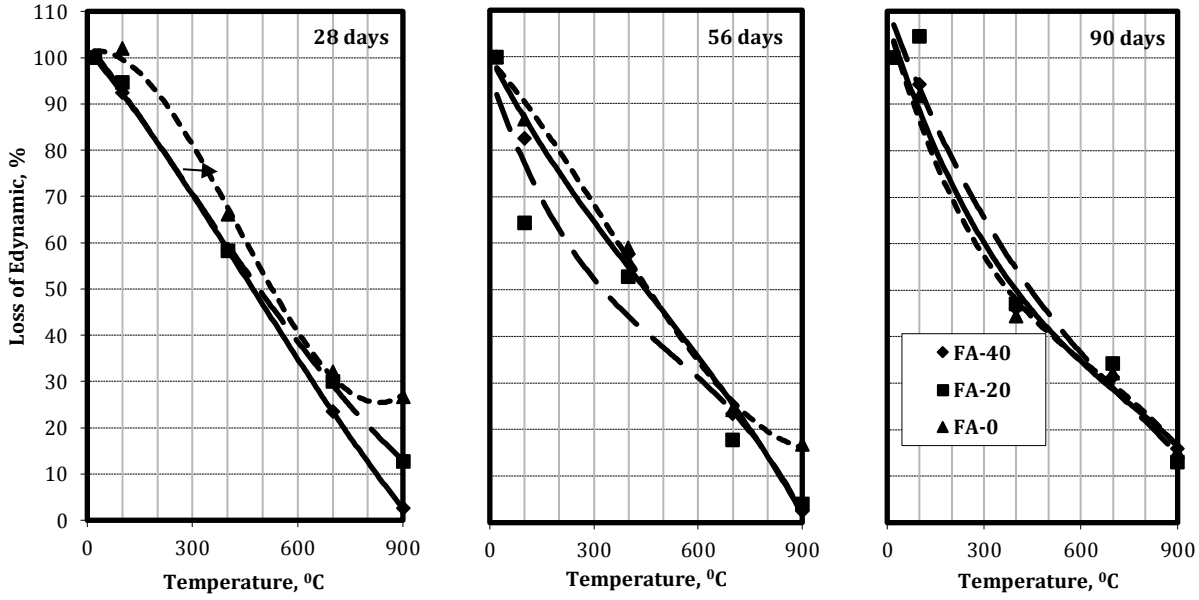

Fig. 12. Relative dynamic modulus of elasticity of SCC at high temperatures.

The strength losses of SCC exposed to high temperatures is shown in Fig. 13. The control specimens that were exposed to 100°C strength decrease by approximately 4%; at 700°C, the loss in the compressive strength increased to 20%. While the temperature increased to 900°C, the loss in strength increased above 60%. At 900°C, the loss of strength for specimens with 20% FA was 45%, whereas the loss of strength for specimens with 40% FA was 65%. With an increase in temperature to 400°C, no significant change was observed in the 28-day compressive strength of specimens. The compressive strength rapidly decreased after 400°C. As the FA did not completely react at an early age and due to the reduction in the coarse aggregate ratio, a significant loss of compressive strength occurred. These losses do not fall below 30%, which provides a significant advantage in terms of the bearing capacity of a structure. The 56-day strength of SCC specimens that were exposed to 400°C increased by 5% when a temperature of 900°C was attained. The loss of strength accelerated to losses over 65%. The loss in strength of specimens, including FA, reached 70% at 900°C. The compressive strength of 56-days specimens decreased at temperatures above 400°C. This reduction, which was similar for the 28-day

specimen, showed similar behaviour by adding FA. A disadvantage of coarse aggregate, which is the decline caused by the acceleration of FA reactions, is eliminated. The compressive strength of 90-day specimens with a maximum temperature of 400°C did not show any change similar to the 28- and 56-days specimens; however, the strength rapidly decreased above 400°C and the strength did not reduce below 45%. The compressive strength positively affected the pozzolanic reaction of FA at high temperatures and even increased at temperatures to 400°C. A minor reduction in the loss of compressive strength at high temperatures was reflected by an increase in the age of concrete.

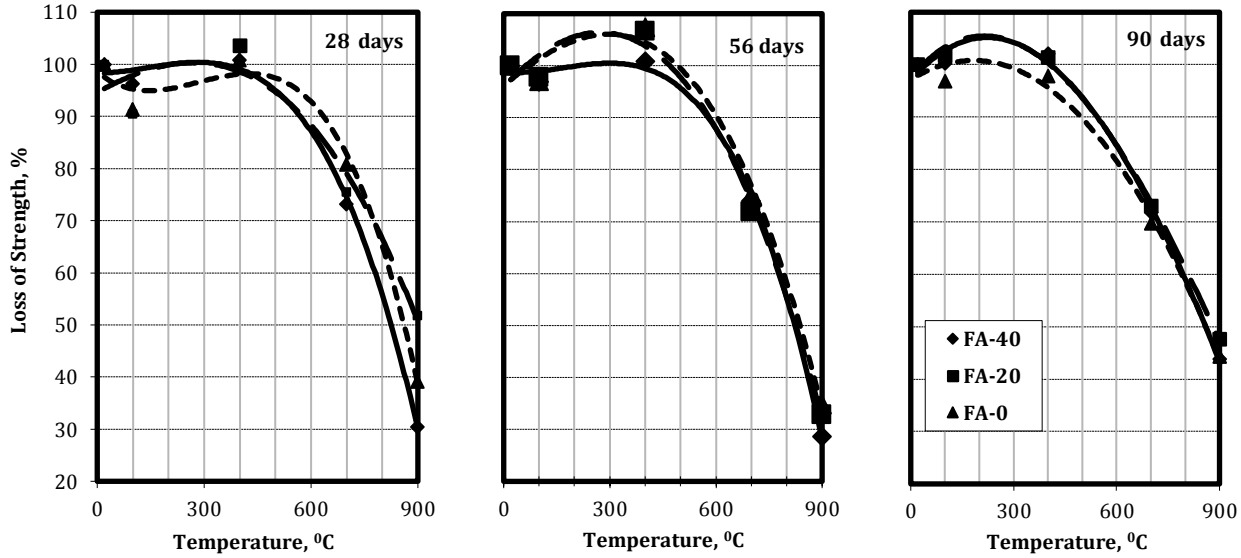

Fig. 13. Relative compressive strength of SCC at high temperatures.

As capillary pores decrease with increasing compactness due to the use of FA, the evaporated water in the microstructure at high temperatures does not easily escape. An increase in internal stress causes micro cracks in concrete, loss of strength and failure. However, compactness decreases the permeability of water and causes less vapor pressure at high temperatures. Growing and branching of these micro cracks were slightly restricted by micro pores, which form with cenosphere FA and plerospher FA, as shown in Fig. 14. It contributes to the elimination of the negative effect of FA on SCC at high temperatures.

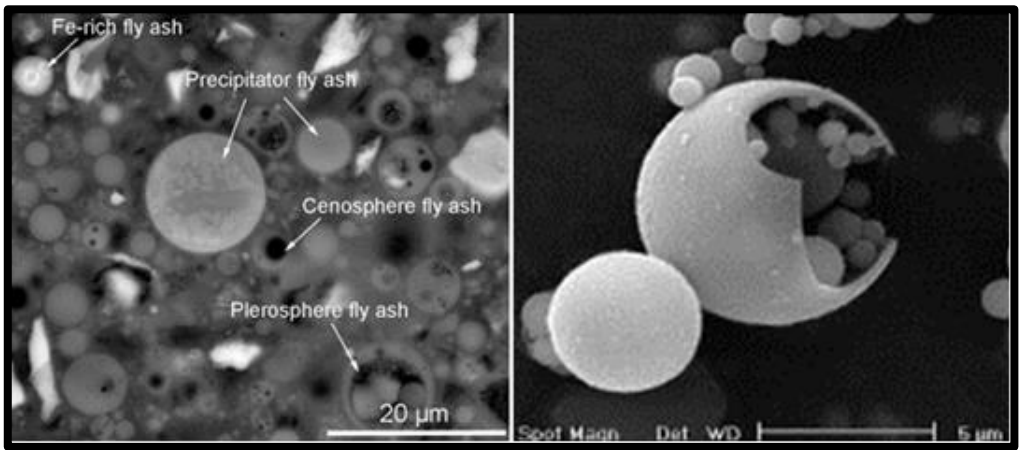

Fig. 14. Microstructure of FA (Patrick et al., 2011; Sujing and Wei, 2014).

4. Conclusions

The conclusions of the study are summarized as follows:

- The decrease in unit weight is dependent on the increase in FA amount in fresh SCC. The filling ability, passing ability, and segregation resistance of SCC are positively affected by increasing the FA amount in fresh SCC.
- An increase in the FA ratio decreases the unit weight of hardened SCC, and unit weight is not affected by concrete age. Although the UPV increases with the age of concrete, the UPV decreases by approximately 6% with the addition of FA in the SCC mixture. The dynamic modulus of elasticity is a similar reaction, such as the UPV, in SCC. The compressive strength of SCC increases with concrete age. An increase in the FA amount in hardened SCC causes a decrease in the

compressive strength. When concrete age is considered, the rate of decrease is approximately 4% of SSC, which includes 20% FA, and approximately 10% of SSC includes 40% FA.

- An increase in temperature in SSC causes a maximum decrease in unit weight of 24%. Due to the effect of high temperature, the difference between the unit weight loss of the control specimens and the unit weight loss of FA mixed specimens is less than 2%.
- As a result of UPV losses, the results conclude that high temperature affects SCC specimens, including FA at early ages. The maximum UPV loss is 60% at 900°C.
- The increase in temperature for SCC linearly decreases in the dynamic elasticity modules. Depending on the increase in concrete age, the differences among the dynamic elasticity modules were not observed between the FA specimens and the control specimens.
- Compressive strength loss is not observed for the SCC at temperatures below 400°C. Specimens older than 90 days are more durable with regard to high-temperature effects and their residual strength approaches the 50% ratio. After 90 days, a positive effect of FA in the SCC that is exposed high temperatures is observed.

According to these results, an increase in the FA amount in SCC decreases the compressive strength and positively affects properties of fresh SCC and the loss of compressive strength at high temperatures. The use of FA in SCC is economical and eco-friendly. The use of 20% FA in SCC decreases the compressive strength by 4%, and the use of 40% of FA in SCC causes a maximum decrease in the compressive strength by 10%. When considering strength, self-compaction, cost and environmental effect, a maximum addition of FA of 20% in SCC mixtures is suggested.

REFERENCES

Acay E (2010). Effect of Elevated Temperature on Self Compacting Concrete Containing Fly Ash. *M.Sc. thesis*, Eskişehir Osmangazi University, Eskişehir, Turkey.

Agwa IS, Ibrahim OMO (2019). Fresh and hardened properties of self-compacting concrete containing cement kiln dust. *Challenge Journal of Concrete Research Letters,* 5(1), 13–19.

Akman MS (2000). Damages of structure and principles of repair. UCTEA Chamber of Civil Engineers Press, İstanbul, 177 p.

Alonzo C, Andrade C, Khoury GA (2003). Relating microstructure to properties, course on effect of heat on concrete. International Centre for Mechanical Sciences (CISM), Italy.

Altın M, Çöğürcü M, Döndüren S (2006). An experimental study into the resistance features of self-compacting concrete (SSC). *Journal of Technical-Online*, 3, 77–88.

Apeh JA (2019). Properties of self-compacting concrete containing granite dust particles. *Challenge Journal of Concrete Research Letters*, 10(2) 34–41.

Cülfik MS (2001). Deterioration of bond between cement paste and aggregate at high temperatures. *Ph.D. thesis*, Boğaziçi University, İstanbul, Turkey.

ERMCO (2005). The European guidelines for self-compacting concrete specification, production and use. *The European Ready-mix Concrete Organization*, 10–68.

Felekoğlu B, Türkel S, Altuntaş Y (2007). Effects of steel fiber reinforcement on surface wear resistance of self-compacting repair mortars. *Cement & Concrete Composites*, 29, 391–396.

Felicetti R, Gambarova PG (1998). Effect of high temperature on residual compressive strength of high strength siliceous concretes. *ACI Materials Journal*, 95, 395–406.

Guise SE, Short NR, Purkiss JA (1996). Colour analysis for assessment of fire damaged concrete, concrete repair, rehabilitation and protection. *Proceedings of the International Conference Held at the University of Dundee*, Scotland, UK.

Güçlüer K, Ünal O (2010). Investigation of effect of fly ash content on the concrete compressive strength and permeability. *Electronic Journal of Construction Technologies*, 6(1), 11–18.

Haddad RH, Shannis L (2004). Post-fire behavior of bond between high strength pozzolanic concrete and reinforcing steel. *Construction and Building Materials*, 18, 425–435.

Hana F, Noumowe A, Remond S (2009). SCC subjected to high temperature mechanical and physicochemical properties. *Cement and Concrete Research*, 39, 1230–1238.

Heiza KM (2012). Performance of self-compacted concrete exposed to fire or aggressive media. *Concrete Research Letters*, 3(2), 406–425.

Helal MA, Heiza KHM (2006). Effect of aggregate type on the behavior of thermally treated SCC. *Egyptian Journal of Applied Science*, 21, 68–82.

Jin T, Yong Y (2006). State of arts on durability research of SCC. *The Third China-Japan Joint Seminar for the Graduate Students*, Shanghai, China.

Kamal MM, Etman ZA, Afify MR, Ahmed TI (2017). Feasibility of using self-compacting concrete in civil engineering applications. *Challenge Journal of Concrete Research Letters*, 8(3), 70–83.

Lawson JR, Phan LT, Davis F (2000). Mechanical properties of high performance concrete after exposure to elevated temperatures. *Department of Commerce Technology Administration*, NIST, USA, 35 p.

Leemann A, Munch B, Gasser P, Holzer L (2006). Influence of compaction on the interfacial transition zone and the permeability of concrete. *Cement and Concrete Research*, 36, 1425–1433.

Mathews ME, Anand N, Nandhagopal M (2020). Influence of mineral admixtures on impact strength of self-compacting concrete under elevated temperatures. *In: IOP Conference Series: Materials Science and Engineering*, 872(1), 1–8, IOP Publishing.

Mohammed MK, Dawson AR, Thom NH (2014). Macro/micro-pore structure characteristics and the chloride penetration of self-compacting concrete incorporating different types of filler and mineral admixture. *Construction and Building Materials*, 72, 83–93.

Neville AM (2000). Properties of Concrete. Fourth Edition, Longman Scientific and Technical, New York, USA.

Papayianni I, Valliasis TH (2005). Heat deformation of fly ash concrete. *Cement & Concrete Composites*, 27, 249–254.

Patrick B, Tim J, Kelly B (2011). The internal microstructure and fibrous mineralogy of fly ash from coal-burning power stations. *Environmental Pollution*, 159, 3324–3333.

Phan LT, Carino NJ (1998). Review of mechanical properties of HSC at elevated temperatures. *Journal of Materials in Civil Engineering*, 10, 58–64.

Poon CS, Azhar S, Anson M, Wong YL (2001). Comparison of the strength and durability performance of normal-and high-strength pozzolanic concretes at elevated temperatures. *Cement and Concrete Research*, 31, 1291–1300.

Savva A, Manita P, Sideris KK (2005). Influence of elevated temperatures on the mechanical properties of blended cement concretes prepared with limestone and siliceous aggregates. *Cement & Concrete Composites*, 27, 239–248.

Scherefler BA, Gawin D, Khoury GA, Majorana CE (2003). Course on effect of heat on concrete. *Physical, Mathematical & Numerical Modelling*, International Centre for Mechanical Sciences, Udine, Italy.

Sujing Z, Wei S (2014). Nano-mechanical behavior of a green ultra-high performance concrete. *Construction and Building Materials*, 63, 150–160.

Topcu İB, Uygunoğlu T (2009). Thermal expansion of self-consolidating normal and lightweight aggregate concrete at elevated temperature. *Construction and Building Meterials*, 23, 3063–3069.

Vodak F, Trtik K, Kapickova O, Hoskova S, Demo P (2004). The effect of temperature on strength-porosity relationship for concrete, *Construction and Building Materials*, 18, 529–534.

Ye G, Liu X, DeSchutter G, Taerwe L, Vandevelde P (2007). Phase distribution and microstructural changes of self-compacting cement paste at elevated temperature. *Cement and Concrete Research*, 37, 978–987.

Challenge Journal of Concrete Research Letters

Research Article

Application of an artificial neural network for predicting compressive and flexural strength of basalt fiber added lightweight

Gokhan Calis [a,*], Sadık Alper Yıldızel [a], Ulku Sultan Keskin [b]

[a] *Department of Civil Engineering, Karamanoğlu Mehmetbey University, 70100 Karaman, Turkey*
[b] *Department of Civil Engineering, Konya Technical University, 42250 Konya, Turkey*

ABSTRACT

Concrete is known as one of the fundamental materials in construction with its high amount of use. Lightweight concrete (LWC) can be a good alternative in reducing the environmental effect of concrete by decreasing the self-weight and dimensions of the structure. In order to reduce self-weight of concrete artificial aggregates, some of which are produced from waste materials, are utilized, and it also contributes to develop a sustainable material Artificial neural networks have been the focus of many scholars for long time with the purpose of analyzing and predicting the lightweight concrete compressive and flexural strengths. The artificial neural network is more powerful method in terms of providing explanation and prediction in engineering studies. It is proved that the error rate of ANN is smaller than regression method. Furthermore, ANN has superior performance over nonlinear regression model. In this paper, an ANN based system is proposed in order to provide a better understanding of basalt fiber reinforced lightweight concrete. In the regression analysis predicted vs. experimental flexural strength, R-sqr is determined to be 86%. The most important strength contributing factors were analyzed within the scope of this study.

ARTICLE INFO

Article history:
Received 18 August 2020
Revised 13 November 2020
Accepted 19 December 2020

Keywords:
Lightweight concrete
Basalt fiber
Artificial neural network
Compressive strength
Strength prediction

1. Introduction

Concrete is known for its high standard of use as one of the essential building materials. It is widely used in buildings, hydraulic structures, and pavements (Calis and Yıldızel, 2019). Due to its high consumption, the normal weight aggregates (NWAs), such as granite and gravel, in construction concrete, natural stone deposits have decreased dramatically. Such amount of use caused non-recoverable damages to the natural environment in the past and goes on. Consequently, the need for sustainable materials has become apparent in recent years (Alengaram et al., 2013).

Lightweight concrete (LWC) can be a good alternative in reducing the environmental effect of concrete by decreasing self-weight and dimensions of the structure. To reduce self-weight of concrete artificial aggregates, some of which are produced from waste materials, are utilized, and it also contributes to developing a sustainable material (Zi et al., 2014). LWC is defined as a versatile material, and it received great attention from the whole construction industry in recent years. LWC can be also utilized as structural concrete, which makes it important material in the modern construction industry. In this respect LWC has been able to solve durability and weight problems in many building and exposed structures (Jafari and Mahini, 2017). Oven dry density of LWC is at the range of 300-2000 kg/m^3 and compressive strength of a cube is from 1 to 60 MPa (Hamad, 2017).

Strength of LWC is as important as it is for conventional concrete. Hence, LWC is required to meet specific strength requirements which can be different depending upon the project. To increase properties of LWC, fibers are commonly used by the scholars. Influences of fiber on mechanical properties of LWC has been investigated by the researchers (Alengaram et al., 2017; Lv et al., 2015; Zhou and Brooks, 2019). These fibers can be mainly divided in to 3 main type: metallic, synthetic and

* *Corresponding author*. Tel.: +90-338-226-2000 ; Fax: +90-338-226-2023 ; E-mail address: gokhancalis@kmu.edu.tr (G. Calis)
ISSN: 2548-0928 / DOI: https://doi.org/10.20528/cjcrl.2021.01.002

natural. Carbon, glass, steel, rubber, waste cable steel and glass are widely used fibers. Among others steel fibers (SF) are mostly used to increase the compressive strength of both normal and lightweight concrete (Wu et al., 2019). Recent studies report that compressive strength can be increased by adding SF. Furthermore, flexural strength and splitting tensile increase significantly (Alengaram et al., 2017; Libre et al., 2011). LWC is known with its low shear capacity in comparison to normal weight concrete. Fiber addition can develop this weak property of LWC. The impact of steel fibers on LWC shear behaviour has been reviewed and concluded that; 0.5% SF addition increased shear resistance from 50.7 kN to 76.6 kN which is 51%. Similarly, when SF addition is 1.0%, the shear resistance enhanced 68% (Mo et al., 2017).

There is limited number of researches on the utilization of glass fiber in LWC. However, it is reported that LWC, which contains 0.06% glass fiber, show 7-11% higher compressive strength than 0% glass fiber added LWC (Hamad, 2017). The compressive strength difference increases by higher level of GF addition. Similarly, another study shows that with GF usage of 0.00 to 0.06%, the compressive strength increases remarkably from 57.85 MPa to 66.01 MPa (Hilles and Ziara, 2019). Also, it is determined that when the amount of GF is higher than 0.06%, the increase of compressive strength is insignificant. Splitting tensile, on the other hand, has increase trend with the increase of GF from 0.00% up to 1.2%. The increase on splitting tensile is higher than compressive strength.

Researchers (Fashandi et al., 2018) investigated the effect of carpet wastes in LWC. It was observed that compressive strength reduces 5.39 %, 8.49% and 14.76% with the use of carpet waste with 1%, 2% and 3%. Flexural strength shows similar trend with the compressive strength. Change in dry density determined to be from 4% up to 14%. Therefore, utilization of carpet wastes has negative impact on both compressive and flexural strength of the concrete. Water absorption of carpet waste added samples is at the range of 6.8% and 9.3%. Obviously, water absorption of concrete is due to high porosity of carpet wastes and this leads the increment.

The Abrams' water-to-cement (binder) ratio (w/c) formula is world-wide accepted by the scholars. The concept of the Abrams' formula indicates that when w/c ratio decreases the strength of concrete increases, when w/c increases strength decreases. This approach does not consider the other ingredients that can impact concrete strength though (Yeh, 1998). It was proved that other ingredients such as silica fume and fiber additions have also impacts on concrete specimen strength (Bhanja and Sengupta, 2005). The current empirical equations compute compressive strength (CS) by investigating the test results without considering supplementary cementitious materials. However, the impact of these supplementary materials such as fibers, fly ash, basalt furnace on compressive strength should also be reviewed (Bhanja and Sengupta, 2005; Yildizel and Calis, 2019). Concrete properties are also influenced by other parameters: quality and quantity of aggregate, cement type (Chopra et al., 2019) .In order to get better understanding regarding the nature of the concrete and optimise the concrete design, concrete composition should be investigated in deep (Castelli et al., 2013). Fiber distribution in concrete mixtures makes difficult to understand and predict compressive strength of concrete mixtures (Altun et al., 2008). Traditional approaches used to determine effect of the parameters on concrete mechanical properties based on analytical equation which fails to get a deep view of it (Getahun et al., 2018). Therefore, the need for generating better solution has grown. In this study basalt fiber added lightweight concrete compressive and flexural strength is investigated by modelling artificial neural networks.

Neural networks have been employed in various fields including structural and engineering problems (Altun et al., 2008). These networks aim to model human brain and perform some of its actions. Neural networks (NN) originally come from mathematical neurobiology. NN are beneficial in predicting and classifying problems. In fact, for these types of problems regression models or some other statistical techniques are also used (Paliwal and Kumar, 2009). NN was investigated in terms of statistical aspects and classified as type of flexible nonlinear regression method. NN is capable of recognizing patters from the past data when it is properly structured and trained (Lenard et al., 1995). Multiple regression, discriminant analysis and logistics regression are the traditional techniques that widely used in prediction and classification problems. NN have gained importance in the recent years, and consequently become alternative solution to the traditional methods in prediction and classification problems (Ripley, 1994).

Artificial neural networks can be considered as purely data driven model that through training iteratively transition from a random state to a final model (Smith and Mason, 1997). Even combination of various algorithms can be used via NN (Behnood and Golafshani, 2018; Yan and Lin, 2016; Yildizel et al., 2020). The recent study reviewed some features of cost estimation model namely; stability, ease and performance in a car manufacturing industry. These features have been investigated by using regression analysis method and neural networks. According to the results, NN have certain benefits in handling data which do not comply with general low order polynomial forms or, which do not have the appropriate cost estimation relationships (CER) for regression modeling with data for which a prior is not very knowledgeable. When sufficient cost estimation relationship data is available, regression models are significantly advanced in predicting (Smith and Mason, 1997). In the other study (Lee et al., 2005), the relationship between welding parameters and geometry of the backbead in arc welding was investigated. Numerous ANN's along with regression analysis methods were utilized in order to perform prediction of the relationship. It was concluded that the error rate predicted by ANN is smaller than the prediction of multiple regression analysis. Scholars concluded that ANN is more powerful in terms of providing explanation and prediction. Furthermore, ANN easily explores the relationships between the data that cannot be understood by the traditional methods (Dvir et al., 2006). In other study, the factors that have impact on the object-oriented (OO) component size

and source code documentation was questioned. Author reviewed the performance of both nonlinear artificial neural networks predicting model and linear regression model. According to the results obtained in the study, when variable returns to scale economies exist between multiple inputs and multiple outputs, ANN has superior performance over nonlinear regression model (Pendharkar, 2006).

Researchers utilized artificial neural networks to understand hybrid steel systems (Allahyari et al., 2018). In their study 90 records was reviewed. The data classified under 2 classes namely training and test. The "train" dataset which has 76 out of 90 records, is utilized in updating the network weight and biases, and computing the gradient. The error of test dataset is not used in the training process, and yet it is still useful to compare different models (Lee and Lee, 2014).

ANN and genetic algorithm in risk optimization of supply chain management were also investigated (Nezamoddini et al., 2019). In that study a typical supply chain structure that contains; supplier, manufacturing plant, distribution center and end user/market was reviewed, and genetic learning algorithm and ANN was used. Nonlinear chance-constrained model in which the uncertainties in center disruption, demand, transaction times, capacity failure, price were taken in to account. The objective function was to maximize net profit by minimizing the initial costs and increasing the market demand.

GEP is an advanced algorithm which includes the idea that the single linear chrome is of a fixed length used in genetic algorithms as well as the structure of the tree, in various sizes and shapes, used for genetic programming. GEP can be considered as a new subarea of GP, which basically contains function set, fitness function, control parameters, terminal set, and termination condition. The main difference between GP and GEP is the way solution is represented in (Jafari and Mahini, 2017).

In other study it was (Tanyildizi and Cevik, 2010) aimed to get empirical genetic programming formulas to predict both compressive and splitting strength of lightweight concrete contains silica and exposed to high temperature. The formulas have been produced by training sets. In their study, properties of genes and functions such as length, number, type of lining, have been selected for each problem. During the solution process, the user is able to start with a single-gene chromosome and then in the later stage this can be increased (Tanyildizi and Cevik, 2010).

A new structured was developed to for prediction of TBM jamming risk in squeezing ground by using Bayesian and ANN (Hasanpour et al., 2019). As part of neural network transaction method if any error occurs in the training this goes backward. This is called backpropagation which is mainly useful in minimizing errors.

Sahar and others (Mohammadi and Nazemi, 2020) studied in management area and analyzed a whole portfolio of projects in terms of value, uncertainty of returns and value by using ANN. Zhang established a model to asses investment risks (Zhang, 2020) and other studies reviewed the prediction of compressive strength of concrete (Duan et al., 2013; Getahun et al., 2018), the other study investigates predicting of lightweight foamed concrete by using ANN (Yaseen et al., 2018).

This study aims to analyze flexural and compressive strength of basalt fiber added lightweight concrete containing ground calcium. In the laboratory part various concrete specimens were tested. The obtained data from the laboratory tests were computed in ANN. In this study 170 samples were prepared, and 17 number of various mixture design were prepared and tested in the laboratory.

2. Materials and Method

2.1. Materials

In the experimental study fine aggregate (FA), also known as river sand, Pumice Aggregates (PA), Betocarb (GCC) and CEM I 42.5 R Cement were utilized. The particle size distributions of the combined aggregates can be seen in Fig. 1.

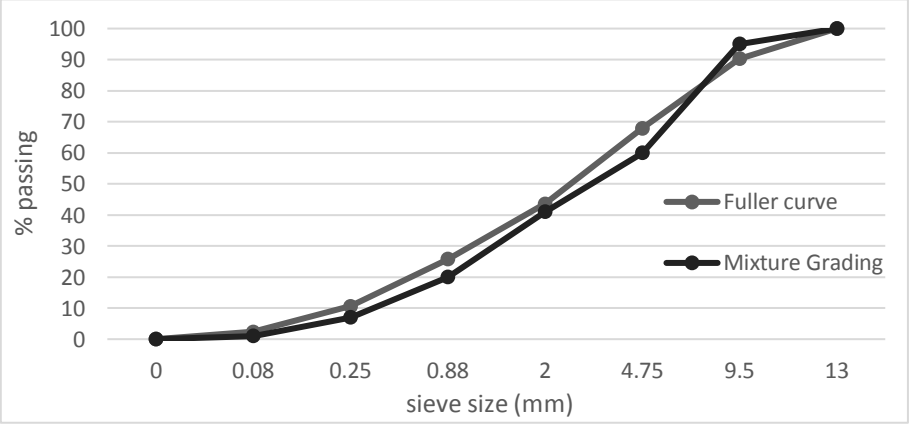

Fig. 1. Fuller curve and aggregate gradation.

Physical properties of the used aggregates (pumice aggregate PA, fine aggregate FA) and the fibers (basalt fiber BF) are shown in Tables 1 and 2. 6mm length BF was used with the volume of 0.25%, 0.5%, 0.75% and 1% in the experimental study. Physical properties of betocarb (GCC) is shown in the Table 3. Polycarboxylic type hyper plasticizer was included in all mixtures at the rate of 1.25 % of cement by weight.

Table 1. Properties of fiber.

Aggregates/property	FA	PA
Particle size (mm)	0- 4	2-12
Particle density (g/cm³)	2.73	2.21

Table 2. Material properties of BFs.

Technical property	
Elasticity module, MPa	90
Tensile strength, MPa	4832
Melting point, °C	1452
Application temperature, °C	-220/+980
Chemical composition	**Percentages (%)**
SiO_2	51.2-58.9
Al_2O_3	14.5-18.2
Fe_2O_3	5.7-9.6
MgO	3.0-5.4
$FeO + Fe_2O_3$	9.2-14.0
TiO_2	0.8-2.25
$Na_2O + K_2O$	0.8-2.25
Others	0.08-0.14

Table 3. Physical properties and chemical compositions of cement, PA and Betocarb® (GCC).

Material property	Cement	PA	Betocarb® (GCC)
Fe_2O_3, %	3.52	1.5	
CaO, %	60.21	0.2	
SiO_2, %	20.19	75.84	
MgO, %	2.32	0.4	
SO_3, %	2.61	0.5	
Al_2O_3, %	4.32	12.54	
Free CaO, %	1.7	-	
Loss on ignition	2.85	5.63	
Specific gravity	3.12	2.35	
Specific surface (cm^2/g)	3,618	-	>30,000
Blue value	-	-	<3
d50%	-	-	3

Compressive strength tests were performed on the Ø100/100 mm cylindrical specimens according to ASTM C469 standard. Flexural strength tests were conducted with 100 x 100 x 500 mm prismatic samples according to the EN 14651. The specimens for flexural strength (FS) were prepared 100 x 100 x 500 samples then cut into 5 pieces to carry out flexural strength tests. The sample can be seen in Fig. 3.

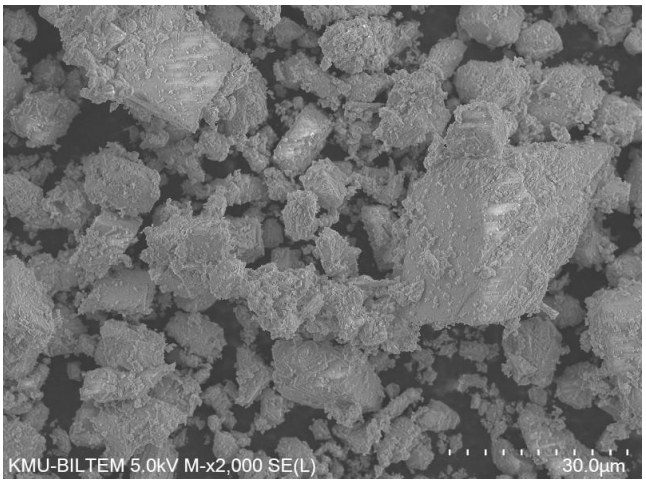

Fig. 2. SEM photo of lightweight concrete.

Fig. 3. Lightweight concrete sample.

2.2. Neural network

In the neural networks 5 variables namely; grounded calcium carbonate (GCC), basalt fiber (BF), Cement (C), fine aggregate (FA), pumice aggregate (PA) are utilized as utilized as input while compressive strength (CS) and flexural strength (FS) are used targets in separate neural networks. Neural network structure is shown in the Fig. 4. The neural network consists of; a scaling layer, a neural network and unscaling layer. The green circles represent scaling neurons, the blue one's perceptron neurons and the orange one unscaling layers. Input values were selected based on the previous experimental test result (Yildizel and Calis, 2019). Levenberg-Marquardt approach were used in this study. This method was designed to reach second - order training speed without having to determine the Hessian matrix (Gavin, 2013). Optimization algorithm is given in Table 6.

The scaling method for this layer is selected by the neural network. The following table shows the values which are used for scaling the inputs, which include the minimum, maximum, mean and standard deviation. Table 4 represents scaling layer and can be seen below.

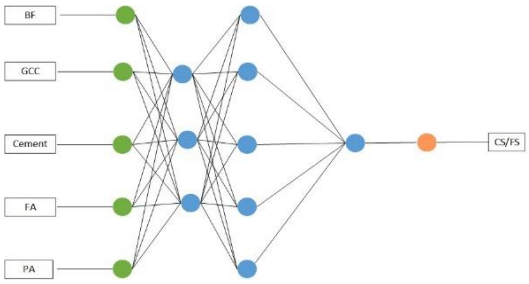

Fig. 4. Neural network.

The size of the unscaling layer is 1, the number of outputs. The un-scaling method for this layer is the minimum and maximum. The following table shows the values which are used for scaling the inputs, which include the minimum, maximum, mean and standard deviation. Data classification of ANN was carried out as proposed: 80% of the data for training and 20% for testing. Unscaling layer can be seen in Table 5.

Basic statistics are very valuable information when designing a model, as they may alert the presence of spurious data. It is necessary to check the correctness of the most important statistical measures of each variable. Table 7 shows the minimums, maximums, means and standard deviations of all the variables in the data set. The scaling layer size is 5, which is the number of inputs.

The norm of the parameters gives a clue as to the accuracy of the predictive model. If the standard parameters are small, the model will be smooth. On the other hand, if the standard parameters are very high, the model may become unstable. Also, it can be noted that the norm depends on the number of parameters. Proposed parameters norms were obtained as 4.19 and 4.24 for compressive and flexural strengths respectively.

Table 4. Scaling layer.

	Minimum	Maximum	Mean	Deviation
BF	0	1	0.588	0.318
GCC	0	25.5	12	9.98
Cement	145	170	158	9.99
FA	741	891	812	58.8
PA	40	450	358	101

Table 5. Unscaling layer.

Minimum	Maximum	Mean	Deviation
14.2	16.7	15.4	0.629

Table 6. Optimization algorithm.

Factors	Description	Value
Damping parameter factor	Damping parameter increase/decrease factor.	10
Minimum parameters increment norm	Norm of the parameters increment vector at which training stops.	0.001
Minimum loss decrease	Minimum loss improvement between two successive epochs.	1e-12
Loss goal	Goal value for the loss.	1e-12
Gradient norm goal	Goal value for the norm of the objective function gradient.	0.001
Maximum selection error increases	Maximum number of epochs at which the selection error increases.	100
Maximum iterations number	Maximum number of epochs to perform the training.	1000
Maximum time	Maximum training time.	3600

Table 7. Data set distribution.

	Minimum	Maximum	Mean	Deviation
BF	0	1	0.59	0.32
GCC	0	25.50	12.01	9.98
Cement	144.50	170	158	9.99
FA	741	891	811.59	58.79
PA	40	450	358.24	100.76
CS	14.21	16.69	15.39	0.63
FS	0.98	1.55	1.32	0.20

3. Results and Discussion

The compressive strength of lightweight concrete is vitally important as it is for conventional concrete. In addition to the environmental effects the ingredients of concrete namely: aggregate, cement, water to cement ratio, existence of fiber, chemical additions, and cement replacement materials. Cement replacement material such as GCC, fly ash perform as filler material and reduce the porosity of concrete. Consequently, the inclusion of such material increases compressive strength (Yildizel and Calis, 2019). In this study it is also proven that GCC has significantly positive impact on the compressive strength of lightweight concrete. It is determined that the optimum amount of GCC is 17 kg for compressive strength as presented in Fig. 6. Cement amount and water to cement (w/c) ratios are another significant factor that impacts the mechanical and durability properties of lightweight concrete. Furthermore, fiber inclusion is another important factor over mechanical properties. Especially, the flexural strength of concrete can be increased by adding basalt fiber as it improves bonding strength.

Regression charts are shown in Fig. 5. R-sqr values were obtained as 84.2% and 86% for estimated compressive and flexural strength respectively, compared to the experimental test results. According to the presented results it is clear that the proposed, ANN model has a good classification and analysing capacity.

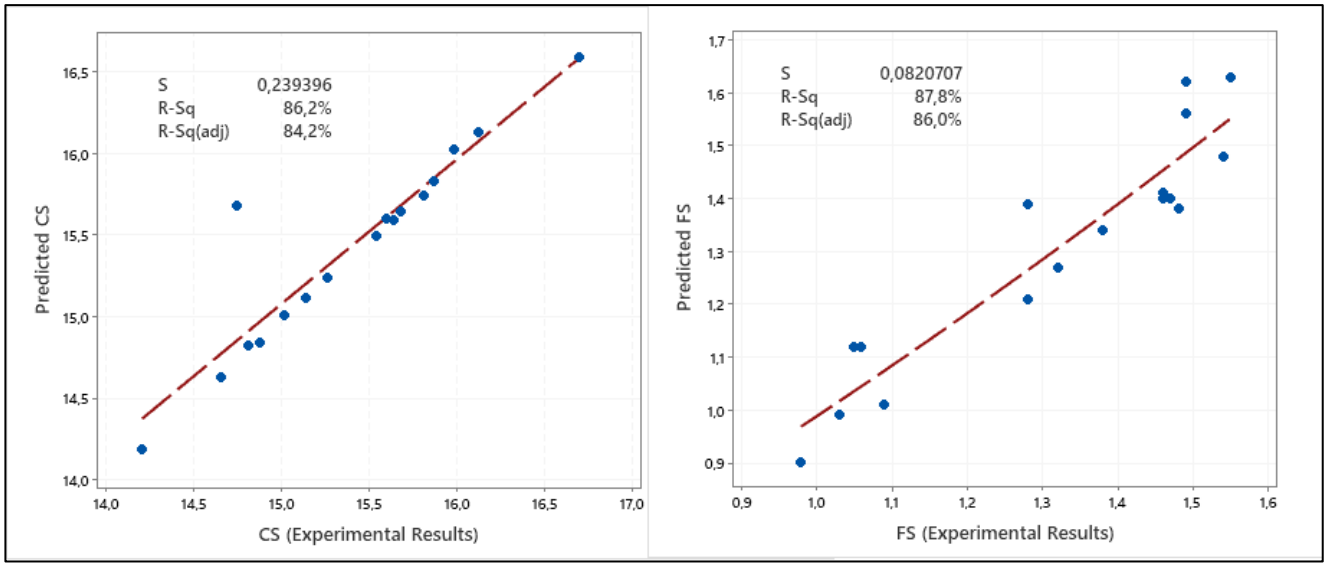

Fig. 5. Experimental results vs. predicted compressive strength (CS) and flexural strength (FS).

Main effects plot for FS and CS are shown in Fig. 6. Samples containing cement content substituted by more than 10 per cent showed lower performance compared to other mixtures. BFs inclusions increased the flexural test results. Mechanical performance improvement of samples can be related to the filler effect of the addition of ground calcium carbonate and basalt fiber to the sample flexural behaviors.

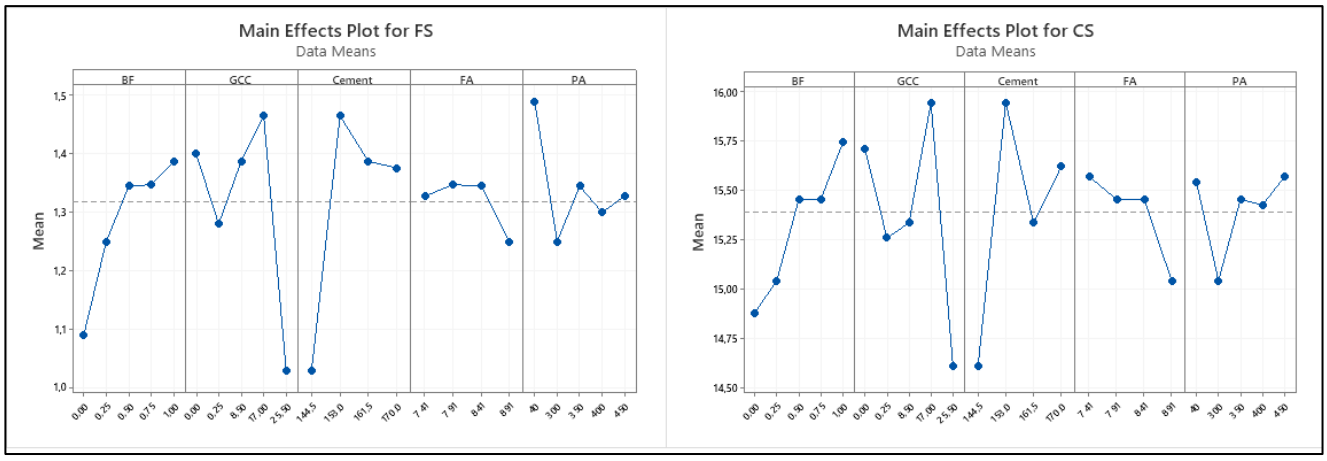

Fig. 6. Main effects plot for FS and CS.

The mathematical expression represented by the neural network is shown in the appendix below. The inputs BF, GCC, Cement, FA, PA are used to compute the output FS. The information is used in propagation in a feed-forward fashion through scaling layer, the perceptron layers and the unscaling layer.

4. Conclusions

The purpose of this study is to develop an ANN based system in order to provide a better understanding for basalt fiber reinforced lightweight concrete. The most important strength contributing factors were analyzed in this research. The outcomes of the research can be drawn as follows:

- As proved earlier by the scholars, the ANN model also approves the strong correlation between the predicted flexural and compressive strengths and experimental test results. In this study, the R-sqr is quite dependable with the value of 84% and 86%.
- Further studies can be carried out with the obtained mathematical equation and applied to the other properties of lightweight concrete.
- The study outcomes can be assessed by other artificial and mathematical systems for improving better ANN-

based systems. More efficient R-sqr values can be obtained by implications of other ANN based systems, which consequently improves the quality of prediction structure.

- Future actions can include the application of the presented methodology to other concrete technologies using the model with new correlation coefficients for estimating.

Appendix

scaled_BF = 2*(BF-0)/(1-0)-1;

scaled_GCC = (GCC-12.0147)/9.97515;

scaled_Cement = 2*(Cement-144.5)/(170-144.5)-1;

scaled_FA = (FA-811.588)/58.7868;

scaled_PA = (PA-358.235)/100.762;

y_1_1 = tanh (0.0152537+ (scaled_BF*-0.912022)+ (scaled_GCC*-2.50899)+ (scaled_Cement*1.40554)+ (scaled_FA*-0.997674)+ (scaled_PA*-2.3887));

y_1_2 = tanh (-0.178526+ (scaled_BF*1.28838)+ (scaled_GCC*-1.46236)+ (scaled_Cement*-0.472198)+ (scaled_Pa*0.54,089));

y_1_3 = tanh (2.18567 + (scaled_BF*1.55428)+ (scaled_GCC*0.130318)+(scaled_Cement*0.566491)+ (scaled_FA*-1.3308)+(scaled_PA*0.492229));

y_2_1 = tanh (-1.40062+ (y_1_1*1.064444)+ (y_1_2*-1.30571)+ (y_1_3*0.467421));

y_2_2 = tanh(-0.367843+ (y_1_1*-1.65566)+ (y_1_2*2.37658)+ (y_1_3*-0.916468));

y_2_3 = tanh (1.80226+ (y_1_1*0.18265)+ (y_1_2*0.10069)+ (y_1_3*-0.916468));

scaled_FS = (-0.181899+ (y_2_1*1.56442)+ (y_2_2*1.60345)+ (y_2_3*1.72238));

FS = (0.5*(scaled_FS+1.0)*(1.55-0.98)+0.98);

References

Allahyari HM, Nikbin I, Rahimi RS, Heidarpour A (2018). A new approach to determine strength of Perfobond rib shear connector in steel-concrete composite structures by employing neural network. *Engineering Structures*, 15, 235–249.

Alengaram UJ, Ghazali NB, Jumaat MZ, Yusoff S, Bashar I, Islam A (2017). Influence of steel fibers on the mechanical properties and impact resistance of lightweight geopolymer concrete. *Construction and Building Materials*, 152, 964–977.

Altun F, Kişi Ö, Aydin K (2008). Predicting the compressive strength of steel fiber added lightweight concrete using neural network. *Computational Materials Science*, 42(2), 259–265.

Behnood A, Golafshani EM (2018). Predicting the compressive strength of silica fume concrete using hybrid artificial neural network with multi-objective grey wolves. *Journal of Cleaner Production*, 202, 54–64.

Bhanja S, Sengupta B (2005). Influence of silica fume on the tensile strength of concrete. *Cement and Concrete Research*, 35(4), 743–747.

Calis G, Yıldızel SA (2019). Investigation of roller compacted concrete: Literature review. *Challenge Journal of Concrete Research Letters*, 10(3), 63–74.

Castelli M, Vanneschi L, Silva S (2013). Prediction of high performance concrete strength using Genetic Programming with geometric semantic genetic operators. *Expert Systems with Applications*, 40(17), 6856–6862.

Chopra P, Sharma RK, Kumar M (2019). Prediction of compressive strength of high-volume fly ash concrete using artificial neural network. *Advances in Materials Science and Engineering*, 25, 471–483.

Duan ZH, Kou SC, Poon CS (2013). Prediction of compressive strength of recycled aggregate concrete using artificial neural networks. *Construction and Building Materials*, 40, 1200–1206.

Dvir D, Ben-David A, Sadeh A, Shenhar AJ (2006). Critical managerial factors affecting defense projects success: A comparison between neural network and regression analysis. *Engineering Applications of Artificial Intelligence*, 19(5), 535–543.

Gavin HP (2013). The Levenberg-Marquardt method for nonlinear least squares curve-fitting problems. *Department of Civil and Environmental Engineering Proceedings,* Duke University, NC, USA.

Getahun MA, Shitote SM, Abiero-Gariy ZC (2018). Artificial neural network based modelling approach for strength prediction of concrete incorporating agricultural and construction wastes. *Construction and Building Materials*, 190, 517–525.

Hamad AJ (2017). Size and shape effect of specimen on the compressive strength of HPLWFC reinforced with glass fibers. *Journal of King Saud University - Engineering Sciences*, 29(4), 373–380.

Hasanpour R, Rostami J, Schmitt J, Ozcelik Y, Sohrabian B (2019). Prediction of TBM jamming risk in squeezing grounds using Bayesian and artificial neural networks. *Journal of Rock Mechanics and Geotechnical Engineering*, 12(1), 21–31.

Hilles MM, Ziara MM (2019). Mechanical behavior of high strength concrete reinforced with glass fiber. *Engineering Science and Technology, an International Journal*, 22(3), 920–928.

Jafari S, Mahini SS (2017). Lightweight concrete design using gene expression programing. *Construction and Building Materials*, 139, 93–100.

Lee K, Booth D, Alam P (2005). A comparison of supervised and unsupervised neural networks in predicting bankruptcy of Korean firms. *Expert Systems with Applications*, 29(1), 1–16.

Lee S, Lee C (2014). Prediction of shear strength of FRP-reinforced concrete flexural members without stirrups using artificial neural networks. *Engineering Structures*, 61, 99–112.

Lenard MJ, Alam P, Madey GR (1995). The Application of Neural Networks and a Qualitative Response Model to the Auditor's Going Concern Uncertainty Decision. *Decision Sciences*, 26(2), 209–227.

Libre NA, Shekarchi M, Mahoutian M, Soroushian P (2011). Mechanical properties of hybrid fiber reinforced lightweight aggregate concrete made with natural pumice. *Construction and Building Materials*, 25(5), 2458–2464.

Lv J, Zhou T, Du Q, Wu H (2015). Effects of rubber particles on mechanical properties of lightweight aggregate concrete. *Construction and Building Materials*, 91, 145–149.

Mo KH, Yeoh KH, Bashar II, Alengaram UJ, Jumaat MZ (2017). Shear behaviour and mechanical properties of steel fiber-reinforced cement-based and geopolymer oil palm shell lightweight aggregate concrete. *Construction and Building Materials*, 148, 369–375.

Mohammadi S, Nazemi A (2020). On portfolio management with value at risk and uncertain returns via an artificial neural network scheme. *Cognitive Systems Research*, 59, 247–263.

Mollahasani A, Alavi AH, Gandomi AH (2011). Empirical modeling of plate load test moduli of soil via gene expression programming. *Computers and Geotechnics*, 38(2), 281–286.

Nezamoddini N, Gholami A, Aqlan F (2020). A risk-based optimization framework for integrated supply chains using genetic algorithm and artificial neural networks. *International Journal of Production Economics*, 3, 110–122,

Paliwal M, Kumar UA (2009). Neural networks and statistical techniques: A review of applications. *Expert Systems with Applications*, 36(1), 2–17.

Pendharkar PC (2006). Scale economies and production function estimation for object-oriented software component and source code documentation size. *European Journal of Operational Research*, 172(3), 1040–1050.

Ripley BD (1994). Neural networks and related methods for classification. *Royal Statistical Society*, 56(3), 409–456.

Smith A, Mason AK (1997). Cost estimation predictive modeling: Regression versus neural network. *Engineering Economist*, 42(2), 137–161.

Tanyildizi H, Çevik A (2010). Modeling mechanical performance of lightweight concrete containing silica fume exposed to high temperature using genetic programming. *Construction and Building Materials*, 24(12), 2612–2618.

Wu T, Yang X, Wei H, Liu X (2019). Mechanical properties and microstructure of lightweight aggregate concrete with and without fibers. *Construction and Building Materials*, 199, 526–539.

Yan F, Lin Z (2016). New strategy for anchorage reliability assessment of GFRP bars to concrete using hybrid artificial neural network with genetic algorithm. *Composites Part B: Engineering*, 92, 420–433.

Yaseen ZM, Deo RC, Hilal A, Abd AM, Bueno LC, Salcedo-Sanz S, Nehdi ML (2018). Predicting compressive strength of lightweight foamed concrete using extreme learning machine model. *Advances in Engineering Software*, 115(3), 112–125.

Yeh IC (1998). Modeling of strength of high-performance concrete using artificial neural networks. *Cement and Concrete Research*, 28(12), 1797–1808.

Yildizel SA, Calis G (2019). Design and optimization of basalt fiber added lightweight pumice concrete using Taguchi Method. *Revista Romana de Materiale/Romanian Journal of Materials*, 49(4), 544–553.

Yildizel SA, Tayeh BA, Calis G (2020). Experimental and modelling study of mixture design optimisation of glass fiber-reinforced concrete with combined utilisation of Taguchi and Extreme Vertices Design Techniques. *Journal of Materials Research and Technology*, 9(2), 2093–2106.

Zhang J (2020). Investment risk model based on intelligent fuzzy neural network and VAR. *Journal of Computational and Applied Mathematics*, 371, 112-125.

Zhou H, Brooks AL (2019). Thermal and mechanical properties of structural lightweight concrete containing lightweight aggregates and fly-ash cenospheres. *Construction and Building Materials*, 198, 512–526.

Zi G, Kim S, Choi J, Hino S,Yamaguchi K (2014). Influence of fiber reinforcement on strength and toughness of all-lightweight concrete. *Construction and Building Materials*, 69, 381–389.

Challenge Journal of Concrete Research Letters

Research Article

Study on concrete proportioning methods: a qualitative and economical perspective

Shoib Bashir Wani [a,*], Tahir Hussain Muntazari [a], Nusrat Rafique [b]

[a] *Department of Civil Engineering, National Institute of Technology Srinagar, J&K 190006, India*
[b] *Department of Geography & Regional Development, University of Kashmir, J&K 190006, India*

ABSTRACT

The various approaches, established for concrete mix design, are not universal because design mixes are explicit to local climate, available materials, and type of exposure. The new-generation mix design method should be developed based on the performance criteria. The concrete strength obtained from the designed concrete mix and optimum cement content should not be considered as the only parameter for the suitability of the concrete mix. This study was carried to compare the proportioning of concrete mixes obtained by following procedures of Indian Standard (IS), American Concrete Institute (ACI) and British Standard (BS) of concrete mix design without the use of admixtures to validate for use in a moderate climate like Kashmir, India. The concrete mixes have been prepared with the necessary 28 days resistance in compression as "15 MPa, 20 MPa, 25 MPa, 30 MPa and 35 MPa". The assessment of water-cement (w/c) ratio; cement, water, fine aggregate (FA) and coarse aggregate (CA) proportion was carried. The w/c ratio among all formulated mixes is significantly high in the BS method and low for IS method. The BS method uses less quantity and IS method uses the maximum quantity of cement. In addition, the ratio of total aggregate content (TAC) and the aggregate-cement ratio is higher in BS design method as compared to IS and ACI design methods. The aggregate content in ACI mix design appears to be consistent and it added to the relative high compressive strength. The specimens cast following BS guidelines failed to attain the target mean strength (TMS) due to a higher volume of aggregate content, high w/c proportion, less quantity of cement in the mix. The specimens cast by ACI and IS mix design upon compression testing showed higher results than the calculated TMS. The cost analysis per cubic meter of concrete revealed that IS and ACI mix proportioning are expensive than BS method. The IS procedure results in dense concrete followed by ACI procedure. It is expected that with a comprehensive investigation on selected design parameters concentrating more on local challenges, the present study will floor the way for the development and adoption of performance-based design mix selection for moderate climate.

ARTICLE INFO

Article history:
Received 10 September 2020
Revised 19 December 2020
Accepted 4 January 2021

Keywords:
Mix design methods
Cement
w/c ratio
Target mean strength
Total aggregate content

1. Introduction

The concrete mix proportioning is a well-defined way of identifying the mixture of ingredients essential to meet the required characteristics in the wet and solidified state. All developed and developing nations have quantified and fixed their concrete mix design procedures. These procedures are largely dependent on tables designed as the outcome of experiments and investigations of material properties, graphs, charts and empirical relations. Many factors found to affect the proportions of ingredients of concrete, such as specific gravity of materials, type and

* *Corresponding author*. Tel.: +91-962-223-8788 ; E-mail address: shoibbwani@gmail.com (S. B. Wani)
ISSN: 2548-0928 / DOI: https://doi.org/10.20528/cjcrl.2021.01.003

strength of cement, the minimum and maximum content of cement, water-to-cement ratio, mixing water requirements, aggregate-to-cement ratio, type, shape and maximum size of aggregates, grading of aggregates, the ratio of fine to total aggregate, entrapped air content, concrete exposure conditions, properties of concrete in green and hardened concrete. All the existing methods of concrete mix formulation follow the same basic trial and error fundamentals. Different methods can be found to design a concrete mixture under requirements that are workability, ingredients and a specific environment. Some of the prevalent approaches of mix design are framed by "Maximum Density Method, Fineness Modulus Method, American Concrete Institute (ACI), Bureau of Indian Standard (BIS), Road Research Laboratory procedure, and Department of Energy (DOE) or British Standard (BS) mix design system" (Raju, 2007). Nataraja et al. (1999) have presented a study from the thorough evaluation of experimental data, tables and graphs developed through in-depth experiments and studies in various mix design procedures. For enhancing the mix design procedures, many functions are noted, and updated mix design parameters have been suggested to generate an economical mixture for varying weather conditions. Mohammed et al. (2012) have proposed an "artificial neural network (ANN)-based design of concrete mixes considering six design parameters, namely w/c ratio, slump, percentage of fine to total aggregate, maximum aggregate size, fineness modulus of fine aggregate, and compressive strength. They concluded that fineness modulus of aggregates has a major effect on the properties of the concrete mix". Lamond (1997) from the analysis of concrete durability has revealed that "durability and strength of concrete are two different parameters; the strength of concrete is just one of the indications of the durability". Wadud and Ahmad (2001) studied the ACI mix design procedure. As per their study, if CA with greater voids is used in making the concrete, it fails to uphold a proper ratio between FA and CA. Al-khalaf and Yousif (1984) have concluded that "the correct proportioning of the aggregate-to-cement ratio is necessary to produce a consistent mix". The DOE method uses the compaction factor as a measure of workability, the ACI method uses the slump. Though the DOE method discusses the air entrainment, the selection of the w/c ratio is a sole function of the target mean strength whereas in ACI method, the determination of the w/c ratio, is a combination of both the target strength and the type of concrete (whether air entrained or non-air entrained).

Nowadays massive concrete structures are constructed worldwide and to assure the safety of life and property, in-depth studies are carried out for promising strength, durability and overall performance of concrete. The present investigation was completed for suggesting the practicality, performance, basic principles of selection and further cost analysis on the concrete mixes formulated by different guidelines. The major drawbacks were included and the suitability for moderate climate conditions was discussed.

2. Summary of Mix Design Procedures

The Indian standard code IS 10262 (2009) presents an elementary assumption that "the compressive strength of concrete is governed by the w/c ratio. The w/c ratio is adopted as per the concrete grade and sort of exposure and water content is selected based on nominal CA size and slump value". The guidelines for the use of any type of admixture in concrete are available. The resilience, w/c proportion and cement quantity requirements are included in IS 456 (2000). The volume of CA is dependent upon the zone of FA as per IS 383 (1970) along with the nominal maximum size of aggregate. The other aspects which influence the property of concrete include the grade and quality of cement; water and aggregate dimensions. Therefore, the instructions mentioned in the proportioning of concrete ought to be considered only as a basis of trial which can be changed. The "compressive strength of hardened concrete is to be specified based on the cube compression test, determined at 28 days" as per IS 516 (1959).

The ACI 211.1 (1991) takes "workability, consistency, strength, and endurance into consideration. ACI suggests mixture design processes based on these principles" (Raju, 2007):

a) In the selection of mix proportion, a wet concrete mix of specified slump comprising a well-graded FA and CA of maximum dimensions will have essentially fixed water content no matter of varying w/c or cement proportion.
b) The w/c proportion is reliant on the concrete strength with a constraint from the durability parameter.
c) The proportion of CA per unit volume of concrete is reliant on the CA size and the FA grading, stated as fineness modulus.
d) Regardless of the process of compaction in concrete, some voids occupy the entrapped air which has indirect proportionality to the maximum dimension of FA and CA.

The disadvantage of ACI method is that for different cement contents the FA cannot be adjusted. There is also no guideline to mix the aggregates of varying sizes. No provisions for lightweight aggregate concrete, special admixtures for manufacturing concrete products and no defined provision for concrete using condensed silica fume. The cement strength perspective is not considered while framing the mix design. "The ACI method of mix design is applicable for normal and heavyweight concrete having 28-days cylinder compressive strength" as per ACI 318-08 (2008).

The BS procedure or Department of Energy (DOE) of concrete mix design method relies on these guidelines (Raju, 2007):

a) The aggregate of two forms of uncrushed and crushed is recognized.
b) Slump values and Vee-bee test time are considered as a measure of the workability of concrete mix.
c) The workability obtained by a specific water-content is proportional to the type of aggregate using different maximum sizes (10 mm, 20 mm, and 40 mm).
d) The FA content is reliant on desired workability, aggregate size and w/c ratio.

The disadvantages of BS method include the FA proportion is greater in the mix design and for varying cement content, the FA cannot be fixed. It doesn't take into account the flakiness of aggregate, FA, water proportion and the effect of aggregate texture. "No specific graphs are recommended to estimate fine aggregate content for a maximum size of aggregates between 10 mm and 20 mm and 20–40 mm. The compressive strength of hardened concrete is to be specified based on 150 mm cube test determined at 28 days in N/mm^2 or 150 mm diameter by 300 mm cylinder tests, determined at 28 days in N/mm^2" as per BS EN 12390-3 (2019).

3. Experimental Program Summary

The concrete mix designs were formulated with basic material properties listed in Table 1.

The sieve analysis results of CA and FA are mentioned in Tables 2 and 3, respectively.

The proportioning of ingredients of a concrete mix by IS, ACI and BS methods are shown in Table 4. The ingredients of the mixes were weighed and casting was carried out using a tilted drum type concrete mixer. Precautions were taken to ensure uniform mixing of ingredients. The specimens were cast in steel moulds and compacted on a table vibrator following IS 516 (1959) guidelines. Cube specimens of size '150mmx150mmx150mm' were cast for cube compressive strength. Curing was done for 28 days by keeping the specimens completely immersed in water. All the test results reported representing the average value obtained from five specimens in each category.

The workability of concrete mix measured in terms of slump and vee-bee is reported in Table 5, including 7th day and 28th day compressive strength.

Table 1. Material properties.

Property		Values
Mean target compressive strength		"15MPa, 20MPa, 25MPa, 30MPa and 35MPa"
Category of cement		Ordinary Portland Cement (OPC) 53 grade, make – Ambuja, in compliance to IS 12269 (1987) was used.
Nominal maximum dimension of CA		20 mm
Category of CA		Crushed natural stone aggregate
Category of FA		River Sand
Specific gravity :	Cement	3.15
	CA	2.62
	FA	2.59
Unit weight of :	CA	1600 kg/m^3
	FA	1700 kg/m^3
Fineness modulus (FM)	CA	7.30
	FA	2.44 (Zone II) as specified in IS 383 (1970)
Water absorption :	CA	0.57%
	FA	1.00 %
Surface moisture :	CA	0.00%
	FA	2.32%
Admixtures		Not used

Note: The experimental temperature was maintained between 25°C to 30°C; a condition of moderate climate temperature.

Table 2. Grading of coarse aggregates.

Sample = 5 kg					
Sieve size		Retained weight (kg)	Collective weight retained (kg)	Collective % retained	Collective % passing
(mm)	(micron)				
80		0	0	0	100
40		0	0	0	100
20		1.519	1.519	30.38	69.620
10		3.444	4.963	99.26	0.740
4.75		0.037	5	100	0
2.36		0	5	100	0
1.18		0	5	100	0
	600	0	5	100	0
	300	0	5	100	0
	150	0	5	100	0
Total Sum		5		729.64	
F M = (729.64/100) = 7.3					

Table 3. Grading of fine aggregates.

Sample = 1000 gram					
Sieve size		Retained weight (g)	Collective weight retained (g)	Collective % retained	Collective % passing
(mm)	(micron)				
4.75		11	11	1.1	98.9
2.36		63	74	7.4	92.6
1.18		141	215	21.5	78.5
	600	245	460	46.0	54.0
	300	214	674	67.4	32.6
	150	326	1000	100.0	0
Total Sum :		1000		243.4	
F M = (243.40/100) = 2.44 , Grading zone II as per IS 383 (1970) (Chaubey, 2020)					

Table 4. Proportioning of ingredients of concrete mix.

Grade of concrete	Standard	Proportion by volume (kg/m^3)			Ratio (Cement:FA:CA)	Water content (litre/m^3)	w/c ratio	Total aggregate-cement ratio
		Cement	FA	CA				
M15	IS	310.00	758.56	1124.92	1:2.44:3.62	182.63	0.59	6.08
	ACI	268.12	862.50	970.00	1:3.21:3.61	180.38	0.80	6.83
	BS	200.00	808.80	1092.00	1:4.04:5.46	165.13	0.86	9.50
M20	IS	338.18	730.02	1129.29	1:2.16:3.34	183.02	0.54	5.50
	ACI	308.33	787.08	1049.60	1:2.55:3.40	180.82	0.59	5.96
	BS	226.67	809.69	1187.00	1:3.57:5.24	166.32	0.73	8.80
M25	IS	372.00	700.90	1130.58	1:1.88:3.03	183.40	0.49	4.92
	ACI	349.06	751.53	1049.60	1:2.15:3.00	181.28	0.52	5.16
	BS	261.54	775.53	1185.51	1:2.96:4.53	166.76	0.63	7.49
M30	IS	413.33	800.62	991.99	1:1.93:2.40	183.78	0.45	4.33
	ACI	411.11	685.44	1115.50	1:1.67:2.71	181.92	0.55	4.38
	BS	283.33	644.38	1079.20	1:2.27:3.80	167.15	0.58	6.08
M35	IS	465.00	767.25	994.50	1:1.65:2.13	183.85	0.40	3.79
	ACI	462.50	560.05	1115.20	1:1.21:2.41	182.50	0.38	3.62
	BS	320.75	384.48	1217.50	1:1.20:3.79	167.57	0.44	4.99

Table 5. Test results.

Grade of concrete	Standard	Slump value (mm)	TMS (MPa)	Mean 7th day compressive strength (MPa)	Mean 28th day compressive strength (MPa)	Average weight of the specimen (kg)
M15	IS	35	20.78	14.67	20.81	8.330
	ACI	30	20.78	14.96	20.89	8.478
	BS	45	20.78	10.81	15.70	8.256
M20	IS	30	26.60	19.56	27.85	8.334
	ACI	35	26.60	19.41	27.78	8.339
	BS	30	26.60	16.81	24.37	8.305
M25	IS	40	31.60	22.30	33.11	8.335
	ACI	30	31.60	23.41	33.48	8.257
	BS	30	31.60	19.41	28.30	8.123
M30	IS	50	38.25	26.52	38.30	8.405
	ACI	30	38.25	26.96	38.59	8.352
	BS	45	38.25	20.44	29.02	8.269
M35	IS	30	43.25	30.81	43.33	8.443
	ACI	30	43.25	30.81	43.26	8.413
	BS	60	43.25	22.37	31.85	8.370

4. Results and Discussion

a) The BS method is comprehensive and tedious, whereas IS and ACI methods are relatively easy and precise.
b) The mix designed by IS and ACI methods attained the calculated TMS and were found to be consistent whereas the trial mixes designed by BS method failed to attain TMS as confirmed by Ejiogu et al. (2018). Fig. 1 displays a bar chart of comparison between 7th day compressive strength, 28th day compressive strength and TMS of all the three concrete mix designs.
c) The w/c ratio is in indirect relation with targeted mean strength in all three methods. The w/c ratio is highest in the BS method, whereas the lowest in IS method. The variation is shown in Fig. 2 (a, b).
d) The proportion of water-content in BS method is less as compared to the other two methods. It is nearly identical in IS and ACI methods. Fig. 3 displays a bar chart of water-content required in different grades of concrete in the respective mix design procedures.
e) The cement-content is directly proportional to the TMS. The IS method utilizes maximum cement proportion and the BS method uses the least which is a factor in the failure of BS mix proportioning method to achieve the TMS. Fig. 4 (a, b) indicates the amount of cement required in the specified concrete mixes as per the respective procedure.
f) The TAC and the aggregate-cement ratio in BS method are high as compared to IS and ACI methods. An indirect relationship between TAC and TMS is observed. Fig. 5 displays a bar chart of the ratio of total-aggregate and cement-content.
g) The CA content is maximum in mixes designed by BS procedure followed by IS and ACI mix designs. No such co-relation in CA content was found in the mixes from low to high TMS.
h) The FA content in IS mix design is inversely proportional to the targeted strength up to M25 and then increases. Whereas in ACI and BS mix design the FA content shows an indirect relationship with the TMS. The consistent proportion of CA: FA in ACI mix designs is a reason for a consistent compressive strength as maximum voids are filled. Fig. 6 (a, b) shows the variation of CA and FA content in different mixes as per IS, ACI and BS method of mix design.
i) The explanation of the failure of BS method is due to high values of w/c ratio, lower cement content and higher quantities of total aggregate than the other two methods. As a result, the proportion of cement appears to be inadequate to cover all the aggregates and bind them properly.

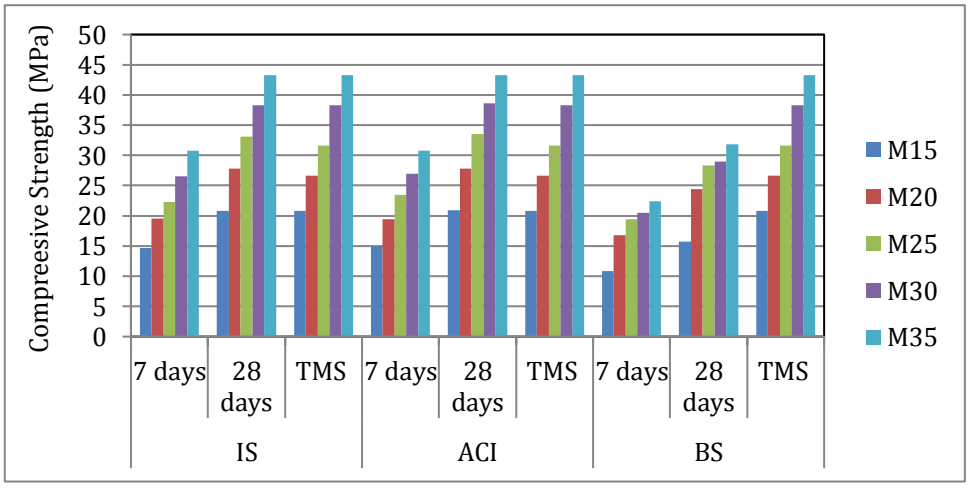

Fig. 1. Comparison of 7th day and 28th day compressive strength and TMS.

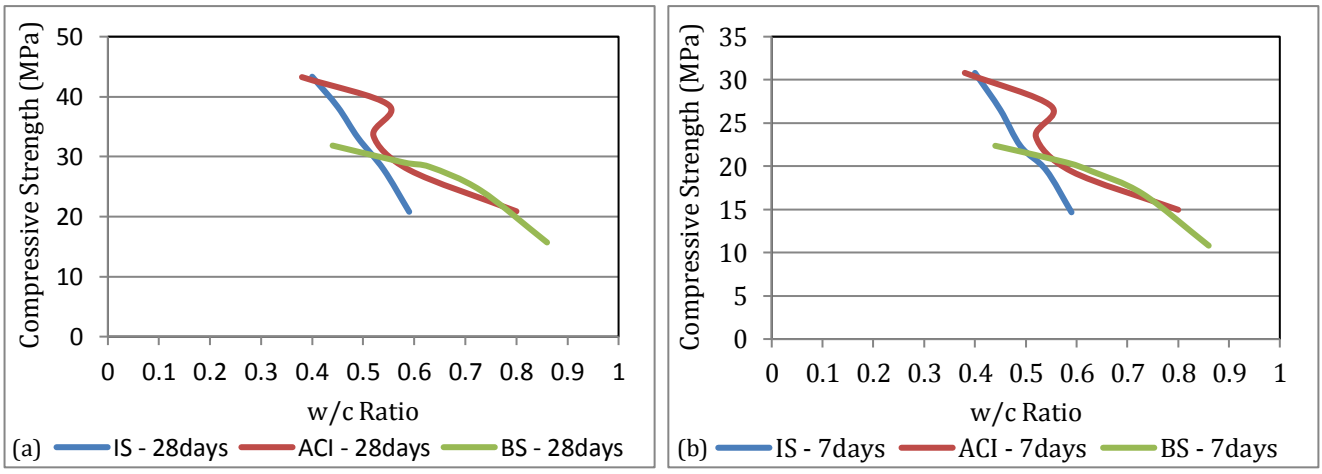

Fig. 2. Compressive strength vs w/c ratio.

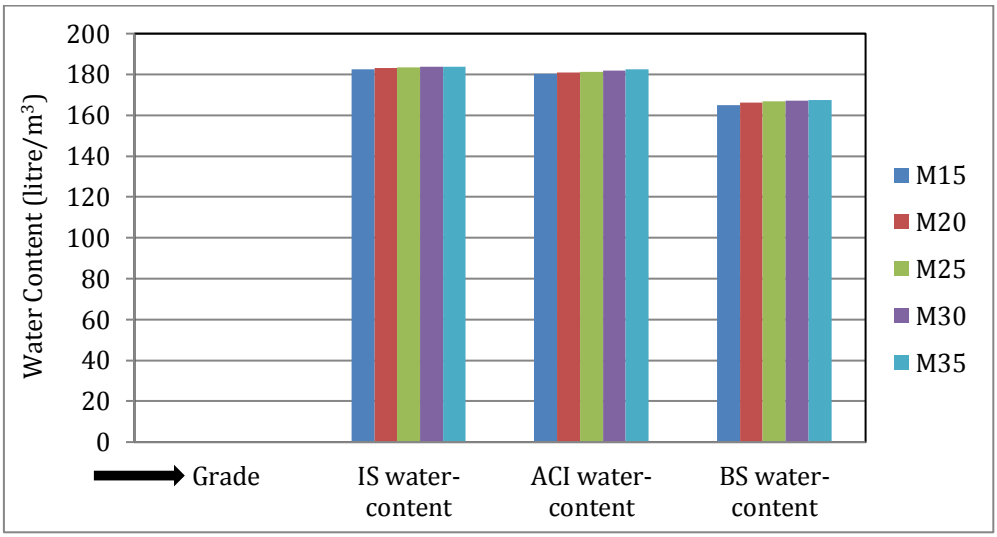

Fig. 3. Water-content required in specified concrete mixes.

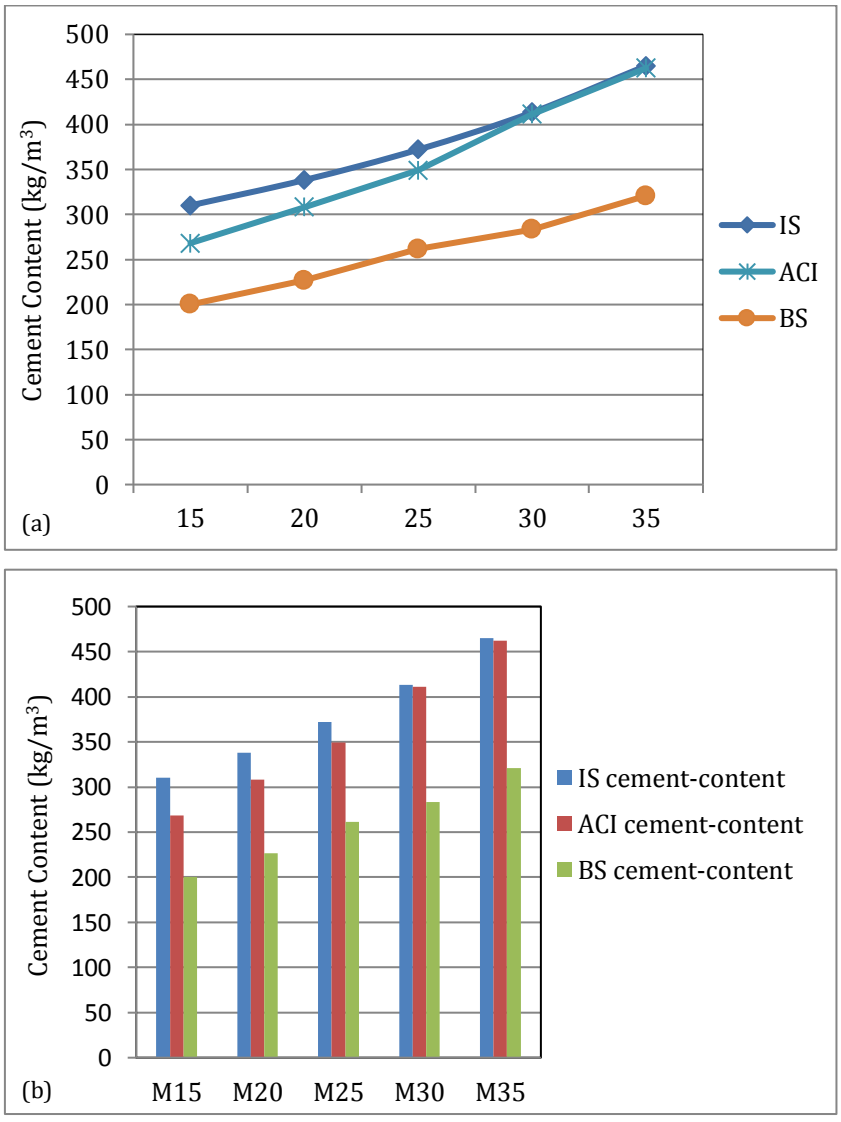

Fig. 4. Variation of cement-content in the designed concrete mixes.

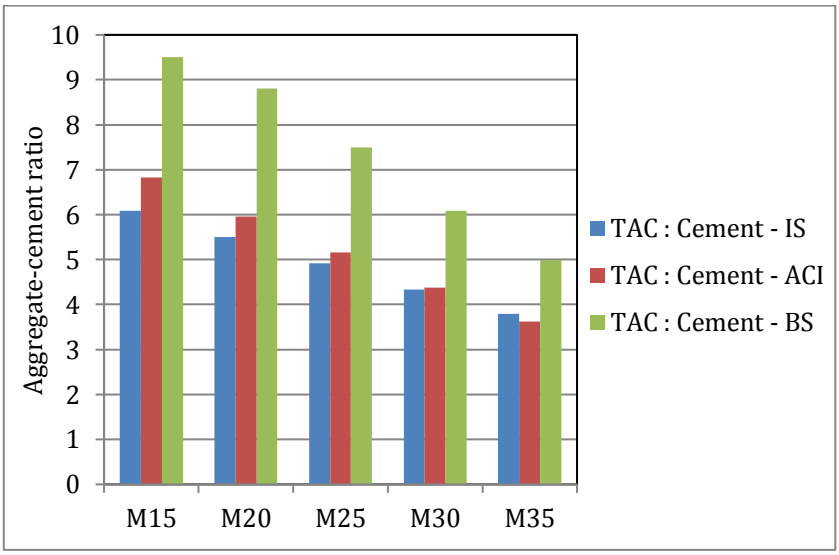

Fig. 5. Total aggregate content- cement content ratio.

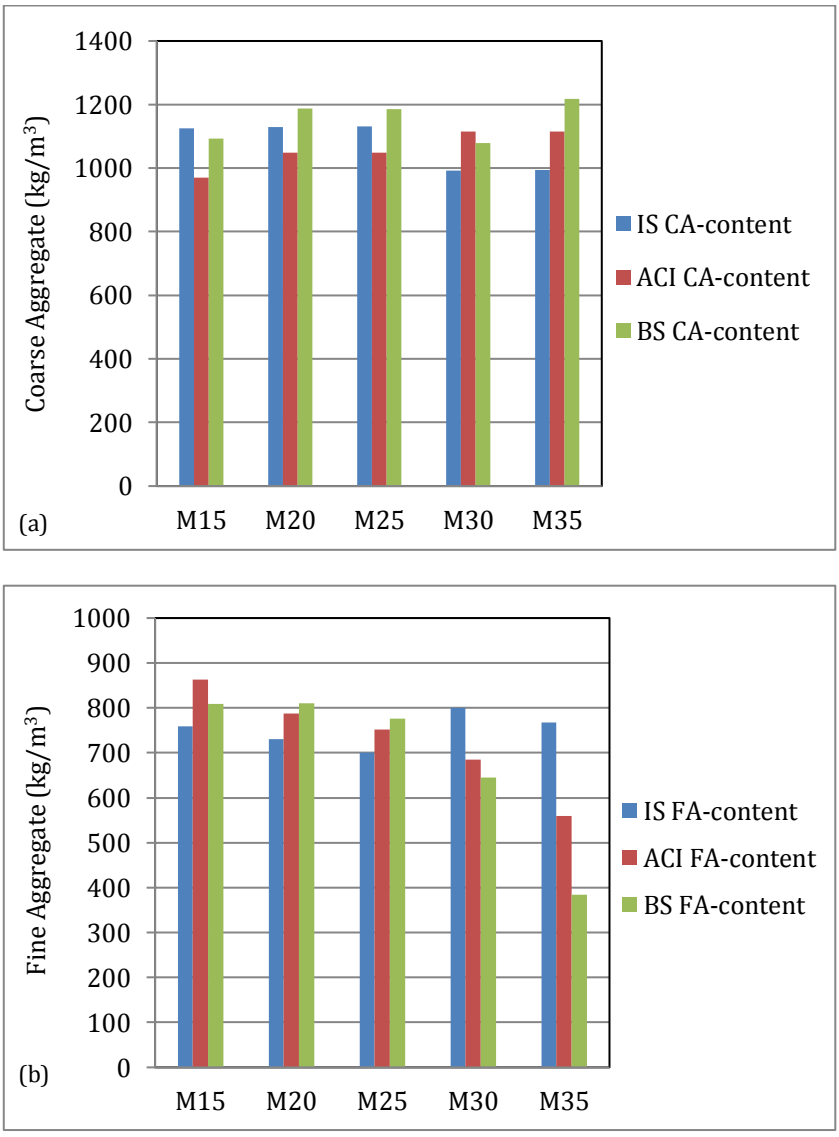

Fig. 6. Variation of coarse aggregate and fine aggregate in designed concrete mixes.

5. Density of Concrete

The "density of the formulated concrete mix was estimated with the attained weight of concrete ingredients per unit volume" (Ahmed et al., 2016) and represented in Table 6. The density of the mix characterizes the compactness of the mix and concrete formed with higher density will be more suitable to harsh conditions.

From Table 6 it is evident that the wet density of fresh concrete and hardened density of concrete specimens (28th day) by mix proportion weight is maximum for IS specimens followed by ACI specimens in all the formulated mix proportions. Therefore, for lower grades of concrete (M15, M20 and M25), ACI concrete proportioning method can be recommended and for higher grades (M30 and M35), IS concrete proportioning method will be more suitable for a moderate climate.

6. Cost Analysis

The basic cost of cement, FA and CA was taken from location Srinagar city (Jammu & Kashmir) as on May 2020. The transportation cost was excluded from the total cost. Table 7 shows the costs of concrete ingredients. The cost per cubic meter of concrete is given in Table 8 and Fig. 7 specifies the cost bar chart.

Table 6. Evaluation of density of fresh concrete and hardened concrete.

Grade of concrete	Standard	Slump value (mm)	Average fresh concrete density	Average weight of the cube specimens (kg)	Average hardened concrete density
M15	IS	35	2297.3	8.33	2468.15
	ACI	30	2261.4	8.478	2512.00
	BS	45	2254.7	8.256	2446.22
M20	IS	30	2369.7	8.334	2469.33
	ACI	35	2343.4	8.339	2470.81
	BS	30	2335.6	8.305	2460.74
M25	IS	40	2384.4	8.335	2469.63
	ACI	30	2352.7	8.257	2446.52
	BS	30	2343.1	8.123	2406.81
M30	IS	50	2387.4	8.405	2490.37
	ACI	30	2359.7	8.352	2474.67
	BS	45	2349.5	8.269	2450.07
M35	IS	30	2399.7	8.443	2501.63
	ACI	30	2368.7	8.413	2492.74
	BS	60	2356.8	8.37	2480.00

Table 7. Material cost.

Material	Cost	Quantity	Unit	Cost of 1kg (₹)
Cement	1500	150	kg	10
FA	2800	2	m^3	1.4
CA	2100	2	m^3	1.05

Table 8. Cost estimation per 1m^3 of concrete.

Grade of concrete	Standard	Cement Qty. (kg/m^3)	FA (kg/m^3)	CA (kg/m^3)	Total Cost per m^3 (₹)
M15	IS	310.00	758.56	1124.92	5343.15
	ACI	268.12	862.50	970.00	4907.20
	BS	200.00	808.80	1092.00	4278.92
M20	IS	338.18	730.02	1129.29	5589.58
	ACI	308.33	787.08	1049.60	5287.29
	BS	226.67	809.69	1187.00	4646.62
M25	IS	372.00	700.90	1130.58	5888.37
	ACI	349.06	751.53	1049.60	5644.82
	BS	261.54	775.53	1185.51	4945.93
M30	IS	413.33	800.62	991.99	6295.76
	ACI	411.11	685.44	1115.50	6241.99
	BS	283.33	644.38	1079.20	4868.59
M35	IS	465.00	767.25	994.50	6768.38
	ACI	462.50	560.05	1115.20	6580.03
	BS	320.75	384.48	1217.50	5024.15

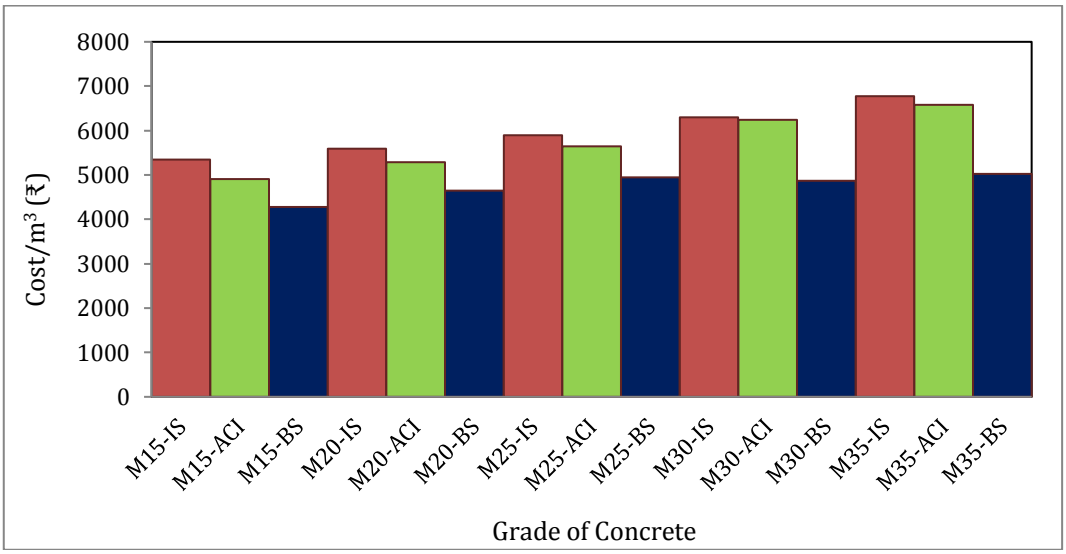

Fig. 7. Graphical representation of cost analysis.

7. Conclusions

Based on the comparative study of mix design procedure as per IS, ACI and BS for quality and economical perspective, the significant conclusions were drawn as follows:

- The method that considers the strength of cement, entrapped air and grading of aggregates with a wide-ranging aggregate size will be more appropriate for the moderate climate conditions as it will yield compact and durable concrete.
- The BS method of mix design is considerably more complex and repetitive and appears to be inconsistent for moderate climate (Kashmir, India).
- The water-content specifies direct proportionality with initial compressive strength and setting time. Less is the water proportion; more will be the 7th day compressive strength and vice versa.
- In the three mix design procedures, the general observations can be summed as: compressive strength is indirectly proportional to w/c ratio; compressive strength shows direct relation with cement-content and indirect relationship with FA content.
- The TAC and the aggregate-cement ratio in BS method are high as compared to IS and ACI methods. This is one of the few reasons for the failure of BS mix design specimens in achieving TMS in 28-days.
- The quality of a concrete mix is determined by the ratio of TAC and cement content. IS and ACI mix design procedures followed indirect relation with TAC and cement ratio from low to high TMS.
- The wet density of fresh concrete and hardened density of concrete specimens (28th day) by mix proportion weight is maximum for IS specimens followed by ACI specimens. For lower grades (M15, M20 and M25) of concrete, ACI concrete proportioning method can be followed and for higher grades (M30 and M35), IS concrete proportioning method can be recommended for a moderate climate.
- The cost analysis per cubic meter of concrete reveals that IS and ACI mix proportioning are costly than BS mix proportioning. The total cost estimation of a concrete mix revealed that cost increases with a decrease in w/c ratio. However, it showed direct proportionality with TMS.

References

ACI 211.1-91 (reapproved 2002). Standard practice for selecting proportions for normal, heavyweight, and mass concrete. American Concrete Institute, USA.

ACI 318-08 (2008). Building code requirements for structural concrete. American Concrete Institute, USA.

Ahmed M, Islam S, Nazar S, Khan RA (2016). A comparative study of popular concrete mix design methods from a qualitative and cost-effective point of view for extreme environment. *Arabian Journal for Science and Engineering*, 41(4), 1403–1412.

Al-khalaf MN, Yousif HA (1984). Concrete Technology Ministry of Higher Education and Scientific Research, University of Technology.

Anon (1946). Laboratory studies of concrete containing air-entraining admixtures. *ACI Journal Proceedings*, 42(2), 305–360.

BS EN 12390-3 (2019). Testing hardened concrete. Compressive strength of test specimens. British Standard Institute, London, UK.

Chaubey A (2020). BRMCA method of proportioning concretes. *Practical Concrete Mix Design*, 97–108.

Chaubey A (2020). ACI method of proportioning concretes. *Practical Concrete Mix Design*, 69–79.

Dewar JD (1995). A concrete laboratory in a computer-case-studies of simulation of laboratory trial mixes. In: *ERMCO-1995, Proceedings of the XIth European Ready Mixed Concrete Congress*, İstanbul, 185–193.

Ejiogu IK, Mamza PA, Nkeonye PO, Yaro AS (2018). Comparative study of various methods for designing and proportioning normal concrete mixture. *The Pacific Journal of Science and Technology*, 19(1), 22–36.

IS 383 (1970). Specification for coarse and fine aggregates from natural sources for concrete (Second Revision). Bureau of Indian Standards, New Delhi, India.

IS 456 (2000). Plain and reinforced concrete – Code of practice (Fourth Revision). Bureau of Indian Standards, New Delhi, India.

IS 516 (1959). Methods of tests for strength of concrete. Bureau of Indian Standards, New Delhi, India.

IS 10262 (2009). Recommended guidelines for concrete mix design. Bureau of Indian Standards, New Delhi, India.

IS 12269 (1987). Specification for 53-grade ordinary portland cement. Bureau of Indian Standards, New Delhi, India.

Lamond JF (1997). Designing for durability. *Concrete International*, 19, 34–36.

Mehta P, de Larrard F (1990). A Method for Proportioning High-Strength Concrete Mixtures. *Cement, Concrete and Aggregates*, 12(1), 47–52.

Mohammed MH, Al-Gburi M, Al-Ansari N, Jonasson JE, Pusch R, Knutsson S (2012). Design of concrete mixes by systematic steps and ANN. *Journal of Advanced Science and Engineering Research*, 2(4), 232–251.

Nataraja MC, Dhang N, Gupta AP (1999). A simple equation for concrete mix design curves of IS 10262:1982. *Indian Concrete Journal*, 73(2), 111–115.

Raju NK (2007). Design of Concrete Mixes, Fourth edition. CBS Publisher, New Delhi, India.

Sobolev KG, Soboleva SV (1996). High strength concrete mix design and properties optimization, concrete technology in developing countries. In: *Proceedings of the 4th International Conference*, Famagusta, TRNC, 189–202.

Wadud Z, Ahmad S (2001). ACI method of concrete mix design: a parametric study. In: *8th East Asia-Pacific Conference on Structural Engineering and Construction*, Nanyang Technological University, Singapore, 1408–1416.

Wani SB, Ahmed J, Mohammed MHS, Muntazari TH, Rafique N (2020). Influence of nano-modification on mechanical and durability properties of cement polymer anticorrosive coating; *Challenge Journal of Concrete Research Letters*, 11(4), p. 92–104.

Wani SB, Haji Sheik MS (2021). Study of bond strength of plain surface wave type rebars with concrete: a comparative study. *International Journal of Engineering, Transactions B: Applications*, 34(2), 326–335.

Zheng SS, Wang XF, Lou HJ, Li ZQ (2011). Optimization design for mix proportioning of high strength and high-performance concrete. *Advanced Materials Research*, 368–373, 432–435.

Challenge Journal of Concrete Research Letters

Research Article

Effect of different fiber types on the mechanical properties of normal and high strength concrete at elevated temperatures

Mohamed Amin [a], Khaled Abu el-hassan [b,*]

[a] *Department of Civil Engineering, Suez University, Suez, Egypt*
[b] *Department of Civil Engineering, Delta University for Science and Technology, Gamasa, Egypt*

ABSTRACT

The effects of the types of fibers on mechanical properties of normal and high strength concrete under high temperature, up to 700 °C, was investigated. Three different- type fiber; "Steel Fiber (SF), Glass Fiber (GF) and Polypropylene Fiber (PPF)" are added into the concretes in five different ratios (0, 0.50, 1.00, 1.50 and 2.0%)of the volume under the following temperatures; 22, 100, 400 and 700°C. The results indicate that all the different types of fibers researched contribute to both the compressive and flexural strengths of concrete under high temperature, however, it is also found that this contribution decreases with an increase in temperature. The flexural strengths and compressive strengths for NSC and HSC mixes at 28 days under high temperature decreases as the temperature increases especially up to 400°C. Also, the best compressive and flexural strengths performance under high temperature was also those of SF. The compressive strength of the concrete incorporating SF was reduced under high temperature only, while the mixes containing PPF and GF were reduced under high temperature or with fiber addition. The optimum fiber addition ratios of the mixes containing PPF and GF are between 0.5-1.0 percent by volume. And for SF, it is 1.5% by the volume.

ARTICLE INFO

Article history:
Received 20 August 2020
Revised 27 February 2021
Accepted 3 March 2021

Keywords:
Steel fiber
Polypropylene fiber
Glass fiber
Compressive strength
Flexural strengths
Elevated temperature

1. Introduction

Fiber reinforced concrete (FRC) may be defined as a composite material made up of cement and aggregate, while incorporating discontinuous fibers. Fibers play a role in is to increase the toughness of the concrete. That is, the fibers tend to increase the strain at peak load, and provide a great deal of energy absorption in the post-peak portion of the load vs. Deflection curve. In recent years, fiber reinforced concrete has become a new way to search and improve mechanical properties and durability of concrete (Juan-García et al., 2016; Zheng et al., 2020; Ghugal and Deshmukh, 2006; Peled et al., 2005; Purnell et al., 2000). Exposure to an elevated temperature may have adverse impacts on mechanical properties of concrete. For the plain concrete, the changes may happen in the pore structures that lead to spalling, cracking, and destroying the ligament between aggregates and cement paste and the decaying of hardening cement paste (Georgali and Tsakiridis, 2005). This process is defined as thermal incompatibility of concrete components and leads to two mechanisms that are the mechanism of build-up vapor pressure (Anderberg, 1997) or the restricted thermal dilatation (Bažant and Kaplan, 1996). Compared to NSC, HSC may be more susceptible to building up pressure that is due to its low permeability (Noumowe et al., 2009; Sanjayan and Stocks, 1993). The dense microstructure of HSC decreases the vapor water and liquid migration. Due to thermal incompatibility, thermal stresses are generated between the cement paste and the aggregate, leading to an induced stress which in turn causes the collapse of the interfacial bond between the aggregate and the cement dough leading to loss of strength (Cülfik and Özturan, 2010). If the concrete is submitted to the fire, free water may be removed in the concrete matrix during a physical process like

* *Corresponding author*. Tel.: +002-0122-316-7385 ; E-mail address: eng_khaled1984@hotmail.com (K. Abu el-Hassan)
ISSN: 2548-0928 / DOI: https://doi.org/10.20528/cjcrl.2021.01.004

evaporation at a lower temperature. With increase in temperature, hydrates disintegration and bonded water loss may occur. Calcium hydroxide decomposition happens approximately at 350°C, while partial volatilization of calcium silicate hydrate gel begins at 500°C. Pore size and porosity of the hydrate matrix may increase, and in turn, mechanical properties like strength and elastic modulus of the hydrates may be decreased. Moreover, the crystal structure of quartz, in a siliceous aggregate at 573 °C, converts from low temperature to a high-temperature phase. This change followed by a one percent volume increase; quickens the hydrates disintegration. All of these transformations make the mechanical properties of a heated concrete (in a macro-scale) depend on the temperature.

Cementitious structures are described as brittle, with decreasing in tensile and flexural strengths. The cementitious structures with fibers resist this weakness; produce the structures with high tensile strength, ductility, toughness and durability. The efficiency of the fibers depends on a multitude of factors including matrix properties, such as size, type, geometry, volume and dispersion of fiber (Kuder and Shah, 2010). Carbon fiber and glass fiber are incombustible materials, therefore their properties are different from polypropylene and polyvinyl alcohol fibers. For decreasing the propagation of crack and increasing the ductility of concrete, these fibers should be added to the concrete mixture. Carbon and glass fibers enhance the mechanical properties of concretes under high temperature that is due to their incombustible properties (Daniel et al., 2002; Pavlík et al., 2002; Şahmaran et al., 2011; Tanyildizi, 2008; Hilles and Ziara, 2019). Studies on the effect of elevated temperature on mechanical properties of fiber reinforced cementitious composites found that the flexural strength of mortar may be significantly improved by different fiber types, but the compressive strength of the mortar reduces under elevated temperatures (Çavdar, 2012; Cree et al., 2017; Mohammadhosseini et al., 2020; Raza et al., 2020).

Altun and Oltulu (2020) investigated the effect of different types of fiber utilization on mechanical properties of recycled aggregate concrete containing silica fume and the results showed that the compressive strength, flexural strength and impact resistance of RAC were reduced as the percentage of RCAs increased. Results of Zhong et al. (2020) showed that the reactive powder concrete ductility can be further improved on the basis of polypropylene fiber RPC, the compressive strength and splitting tensile strength of polypropylene fiber.

The main aim of the current study to investigate the impacts of the different fiber types on the mechanical properties of normal and high strength concretes at elevated temperature. Regarding the novelty of this paper, it is significantly original because it involved analyzing the behaviours of the normal and high strength concretes resulting represented in its compressive and flexural strengths at different degree of temperatures. The production of twenty-six concrete mixtures with three types of fibers and five ratios are made for this purpose. The mixes are submitted to four elevated temperatures. Steel Fiber (SF), Glass Fiber (GF) and Polypropylene Fiber (PPF) are selected for the fibers. These fibers are added to the concrete in five ratios (0, 0.5, 1.0, 1.5 and 2.0%) by volume. The concrete are subjected to elevated temperatures: 22, 100, 400 and 700°C. The mechanical properties investigated are compressive and flexural strengths of the concrete mixes.

2. Experimental Work

In this study, the known effects of the types of fiber on mechanical properties of normal and concrete of high strength under high temperature are investigated. The materials that are used in the present research were selected from local materials in Egypt.

2.1. Materials

Portland cement type CEM I–52.5 N was used in concrete mixes. In accordance with the Egyptian Standard Specification (ES: 4756/1 2013), the cement testing was achieved. The properties of the cement in use are shown in Table 1. Three different fiber types are used in the experimental work. The fibers are SF, GF and PPF. Table 2 reveals the fiber properties used in this work. The aggregates used in this research work consisted of local natural coarse aggregates (crushed dolomite) (4/19) mm with a specific density of 2.68 gm/cm^3, and maximum nominal size of 19 mm and natural siliceous sand (0/4) mm with a specific density of 2.65 gm/cm^3, and fineness modulus of 2.75. The coarse aggregate was washed about forty-eight hour before used and left to dry to prevent the impact of fine materials. According to Egyptian Standard (1109), testing of crushed dolomite and siliceous sand was performed. The silica fume that is used was locally produced in Egypt having 97.6% silica, and a bulk unit weight of 355 kg/m^3. A superplasticizer (SP) admixture of an aqueous solution of modified polycarboxylate basis was used. SP complies with ASTM-C-494 types F and G, with a specific density of 1.08 gm/cm^3.

Table 1. Physical and chemical composition of cementitious materials.

Properties	CEM I	Silica Fume
Physical		
Specific density (gm/cm^3)	3.14	2.13
Specific area (cm^2/gm)	3550	20500
Colour	Grey	Light Grey
Chemical compositions (%)		
Silicon dioxide (SiO2)	20.24	97.60
Calcium oxide (CaO)	62.23	0.25
Aluminium oxide (Al_2O_3)	5.91	0.18
Ferric oxide (Fe_2O_3)	3.34	0.45
Sulphur trioxide (SO_3)	2.19	0.10
Magnesium oxide (MgO)	2.15	0.55
Sodium oxide (Na_2O)	0.82	0.16
Potassium oxide (K_2O)	0.76	0.45
Loss on Ignition (LOI)	1.67	0.60

Table 2. Properties of the fiber types.

Properties	SF	GF	PPF
Length (mm)	15	15	15
Specific mass (kg/m^3)	7800	2600	900
Tensile strength (MPa)	2200	1600	400
Modulus of elasticity (MPa)	200000	71000	4000
Surface texture	Smooth	Grooved	Grooved
Absorption	None	Low	Low
Alkali resistance	High	High	High

2.2. Mix proportion

To achieve the aims of this work, two groups of concrete with a total number of 26 mixtures were prepared and investigated. Table 3 presented the mix design of all mixtures. The mixtures were grouped into two representing the variables in the study. The first group with 350 kg/m^3 cement content (mixes from M1 to M13), mix M1 possesses neither fibers nor silica fume (control mix), while the mixes from M2 to M13 contains three different fiber types with percentages of 0.5, 1.0, 1.5 and 2.0, and a water-cement ratio of 0.60 for mixes (M1 to M13). The second group with 450 kg/m^3 cement content (mixes from S1 to S13), mix S1 possesses neither fibers, while the mixes from S2 to S13 containing three different fiber types with percentages of 0.5, 1.0, 1.5 and 2.0. It contains also silica fume with a percentage of 15 and superplasticizer with a percentage of 3.0 as replacement of cement. The water to binder ratio was equal 0.25 for mixes (S1 to S13).

Table 3. Proportions of concrete mixtures.

Mix	CEM I (kg)	Sand (%)	Dolomite (%)	Silica fume (%)	Superplasticizer (%)	Water (w/b)	Fiber type (%)		
							SF	GF	PPF
M1	350	40	60	0	0	0.6	0	0	0
M2	350	40	60	0	0	0.6	0.5	0	0
M3	350	40	60	0	0	0.6	1.0	0	0
M4	350	40	60	0	0	0.6	1.5	0	0
M5	350	40	60	0	0	0.6	2.0	0	0
M6	350	40	60	0	0	0.6	0	0.5	0
M7	350	40	60	0	0	0.6	0	1.0	0
M8	350	40	60	0	0	0.6	0	1.5	0
M9	350	40	60	0	0	0.6	0	2.0	0
M10	350	40	60	0	0	0.6	0	0	0.5
M11	350	40	60	0	0	0.6	0	0	1.0
M12	350	40	60	0	0	0.6	0	0	1.5
M13	350	40	60	0	0	0.6	0	0	2.0
S1	450	40	60	15	3	0.25	0	0	0
S2	450	40	60	15	3	0.25	0.5	0	0
S3	450	40	60	15	3	0.25	1.0	0	0
S4	450	40	60	15	3	0.25	1.5	0	0
S5	450	40	60	15	3	0.25	2.0	0	0
S6	450	40	60	15	3	0.25	0	0.5	0
S7	450	40	60	15	3	0.25	0	1.0	0
S8	450	40	60	15	3	0.25	0	1.5	0
S9	450	40	60	15	3	0.25	0	2.0	0
S10	450	40	60	15	3	0.25	0	0	0.5
S11	450	40	60	15	3	0.25	0	0	1.0
S12	450	40	60	15	3	0.25	0	0	1.5
S13	450	40	60	15	3	0.25	0	0	2.0

2.3. Test procedures

The compressive strength test of concrete was tested using cubes (150 mm) according to BS 1881: part 116–2004, at the age of 28 days. The flexural strength test at 28 days was performed according to ASTM C78/C78M-16. The prism specimens of 100×100×500 mm for flexural strength were used. The density of concrete at 28 days was performed according to BS 1881: part 114–2004. An average of three specimens was recorded for each testing age and all strengths. The specimens of mixes were demolded 24 hours after the casting and placed in the standard water tank until testing at 28 days. After 28 days water curing, they were heated in an electric furnace up to 100, 400 and 700°C. Each temperature was maintained for 1.5 hours to achieve the thermal steady state. The specimens were allowed to cool naturally to room temperature.

3. Results and Discussion

The results of compressive strength, flexural strength and density of mixes under elevated temperatures are shown in Table 4.

Table 4. Properties of normal and high strength concrete at high temperature.

Mix	Compressive Strength (MPa)				Flexural Strength (MPa)				Density (kg/m³)				Notes
	22°C	100°C	400°C	700°C	22°C	100°C	400°C	700°C	22°C	100°C	400°C	700°C	
M1	33.50	34.82	30.17	16.07	5.34	5.00	1.76	0.96	2260	2260	2170	2130	Control mix.
M2	34.85	38.68	33.46	19.51	5.71	6.68	3.71	1.55	2280	2280	2190	2165	SF-0.5%
M3	36.52	42.36	34.70	19.36	6.30	7.24	4.10	1.64	2300	2300	2208	2186	SF-1.00%
M4	37.86	42.40	35.59	19.68	6.89	8.00	4.41	1.73	2325	2325	2232	2209	SF-1.5%
M5	36.85	40.90	33.53	18.05	6.09	7.07	3.84	1.58	2350	2350	2258	2136	SF-2.00%
M6	28.80	31.40	23.05	12.10	5.50	6.44	2.59	0.83	2145	2145	2037	2017	GF - 0.5%
M7	27.47	31.32	18.41	10.44	5.67	6.35	2.22	0.63	2075	2075	1972	1950	GF - 1.00%
M8	25.12	27.90	11.30	6.28	5.08	5.90	2.29	0.56	1990	1990	1870	1832	GF - 1.5%
M9	23.45	27.44	8.68	4.69	4.55	5.00	2.14	0.46	1900	1900	1768	1713	GF - 2.00%
M10	30.51	32.65	23.50	11.60	5.66	6.68	2.61	0.85	2150	2150	2043	2025	PPF -0.5%
M11	28.13	30.40	20.25	10.41	6.00	6.78	2.16	0.84	2080	2080	1980	1958	PPF -1.00%
M12	26.80	29.50	16.10	10.71	5.35	6.10	1.72	0.59	2060	2060	1960	1937	PPF -1.5%
M13	25.13	29.15	12.10	7.54	4.92	5.41	1.48	0.50	2036	2036	1938	1915	PPF - 2.00%
S1	88.50	90.28	61.95	23.90	14.00	12.88	3.92	1.68	2340	2340	2246	2108	Control mix.
S2	91.16	101.19	82.05	44.66	14.84	17.21	9.35	3.71	2360	2360	2290	2264	SF-0.5%
S3	93.82	106.02	82.56	45.04	16.53	19.00	9.92	3.97	2385	2385	2312	2290	SF-1.00%
S4	98.23	111.98	87.43	46.17	17.64	20.11	10.6	4.42	2410	2410	2330	2314	SF-1.5%
S5	95.58	106.10	83.16	42.06	16.10	18.19	9.67	3.87	2430	2430	2357	2330	SF-2.00%
S6	77.89	84.12	62.32	31.16	14.28	16.57	6.34	2.00	2245	2245	2155	2130	GF - 0.5%
S7	74.34	84.74	47.58	26.77	14.72	16.34	5.74	1.62	2175	2175	2087	2065	GF - 1.00%
S8	68.15	75.00	28.63	15.68	13.17	12.38	5.80	1.32	2100	2100	1996	1950	GF - 1.5%
S9	63.73	72.02	21.03	11.47	11.64	12.57	5.24	1.17	2016	2016	1894	1833	GF - 2.00%
S10	82.31	88.90	60.09	30.46	14.71	17.06	6.62	2.06	2250	2250	2160	2139	PPF -0.5%
S11	76.11	82.20	53.30	26.63	15.55	17.42	5.44	2.02	2180	2180	2095	2070	PPF -1.00%
S12	73.46	79.34	41.87	25.00	13.86	15.94	4.30	1.39	2155	2155	2070	2048	PPF -1.5%
S13	69.03	78.70	31.06	18.64	12.75	14.03	3.57	1.28	2130	2130	2045	2024	PPF - 2.00%

3.1. Compressive strength

The comparison between non-fibrous concrete and mixes incorporating with three distinctive fiber types subjected to four different temperatures. Fig. 1 and Table 4 show the compressive strength of the normal strength concrete mixes under high temperature. It can be seen that the compressive strength of non-fibrous concrete decreases as the temperature increases. The compressive strength of non-fibrous concrete reduces approximately 10% at 400°C and about 52% at 700°C. Compressive strength of SF concrete mix reduces about 10% at 400°C (SF-2.0%) and on average 52% at 700°C (SF-2.0%). While GF, the reduction are about 63% at 400°C (GF-2.0%) and on average 80% at 700°C (GF-2.0%). And for PPF, the reduction is about 52% at 400°C (PPF-2.0%) and about 70% at 700°C (PPF-2.0%). Fig. 2 and Table 4 show the compressive strength of the high strength concrete mixes under high temperature. For non-fibrous concrete, it can be seen that the compressive strength of decreases as the temperature increases. The compressive strength of HSC without fibers decreases on average 30% at 400°C and about 72% at 700°C. The compressive strength of HSC with SF reduces about 13% at 400°C (SF-2.0%) and on average 56% at 700°C (SF-2.0%). But GF, the reduction is about 67% at 400°C (GF-2.0%) and on average 82% at 700°C (GF-2.0%). And for PPF, the decreases are on average 55% at 400°C (PPF-2.0%) and about 73% at 700°C (PPF-2.0%).

The difference between the compressive strength test for normal or high strength concrete (non-fibrous concrete and mixes incorporating with three different fiber types subjected to four different temperatures) is shown in Figs. 3 and 4. Decreases in compressive strength remain at a reasonable level for up to 1.0% fiber addition for each temperature, for all types of fibers. Elevated temperatures, decay the concrete by changing the cement paste hydration. Because of the ductile structure of the fibers compared to the concrete and having the cause of the concrete discontinuity, they are added in the normal strength concretes or high strength concretes. This helps in reducing the compressive strength. According to the samples investigated under dry conditions, around 100°C, fibers revealed better performance comparing to those of wet conditions (22°C). The references show that the melting of fibers at elevated temperatures form gaps that meet the vapor pressure. The findings of the compressive strength at elevated temperatures for all mixes are consistent with the results in the studies of Cülfik and Özturan (2010), Çavdar (2012), Amin et al. (2020), and Mohammadhosseini et al. (2020).

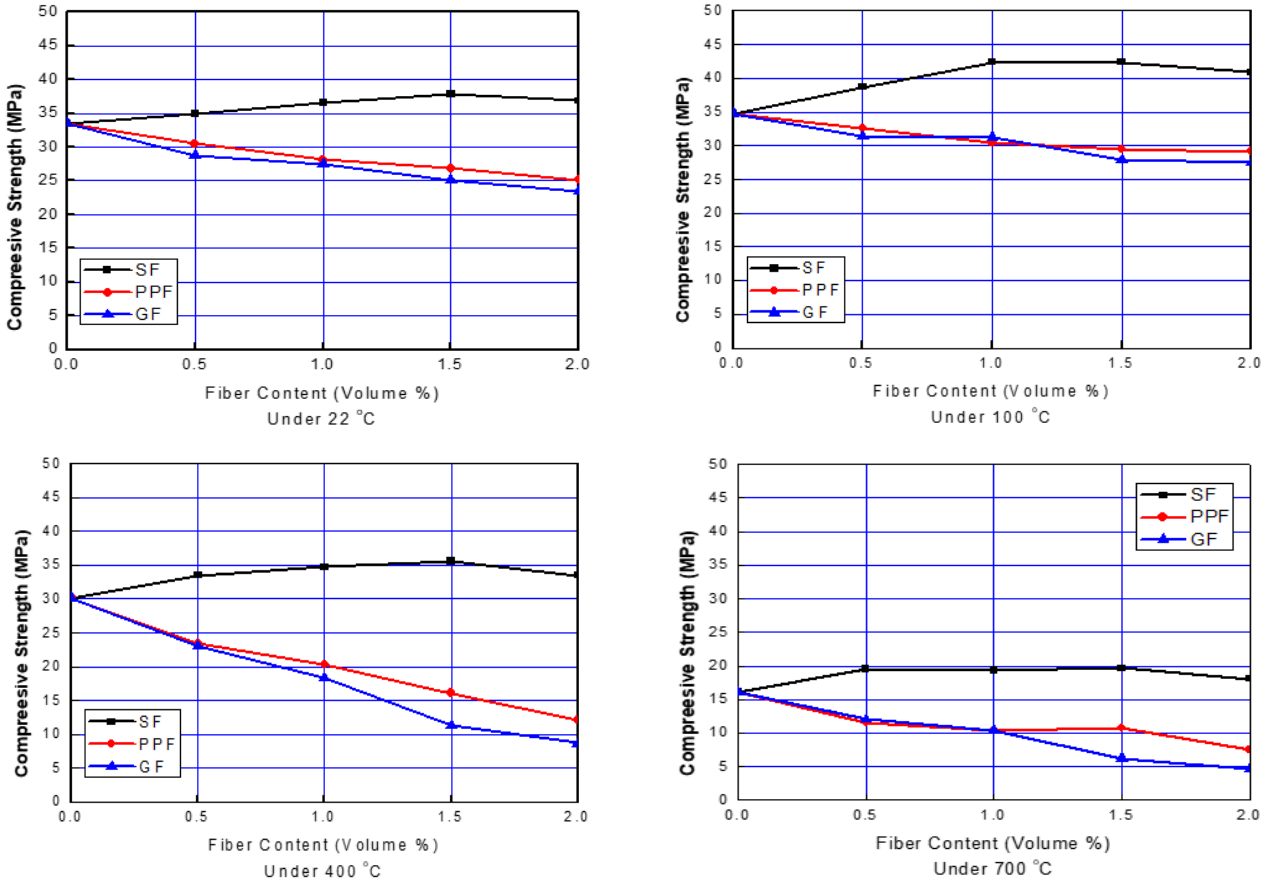

Fig. 1. Effect of fiber content on compressive strength at high temperature (normal strength concrete).

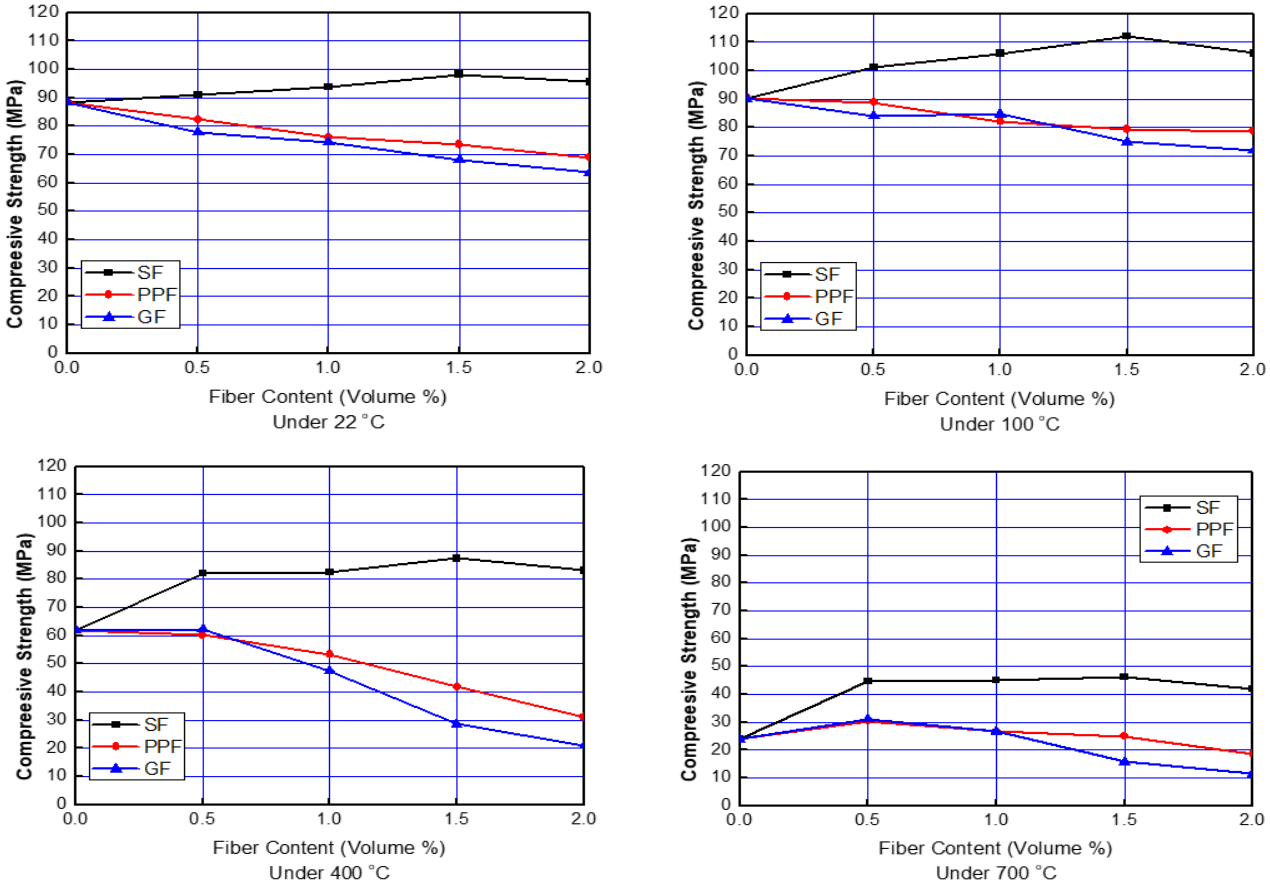

Fig. 2. Effect of fiber content on compressive strength at high temperature (high strength concrete).

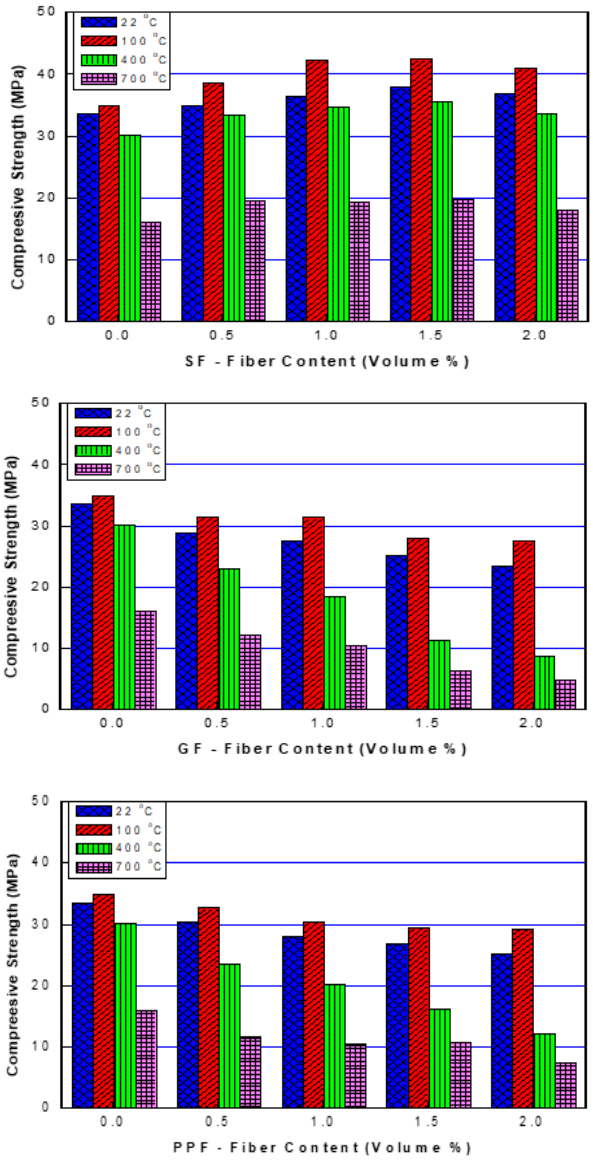

Fig. 3. Effect of fiber content on compressive strength at different temperatures (normal strength concrete).

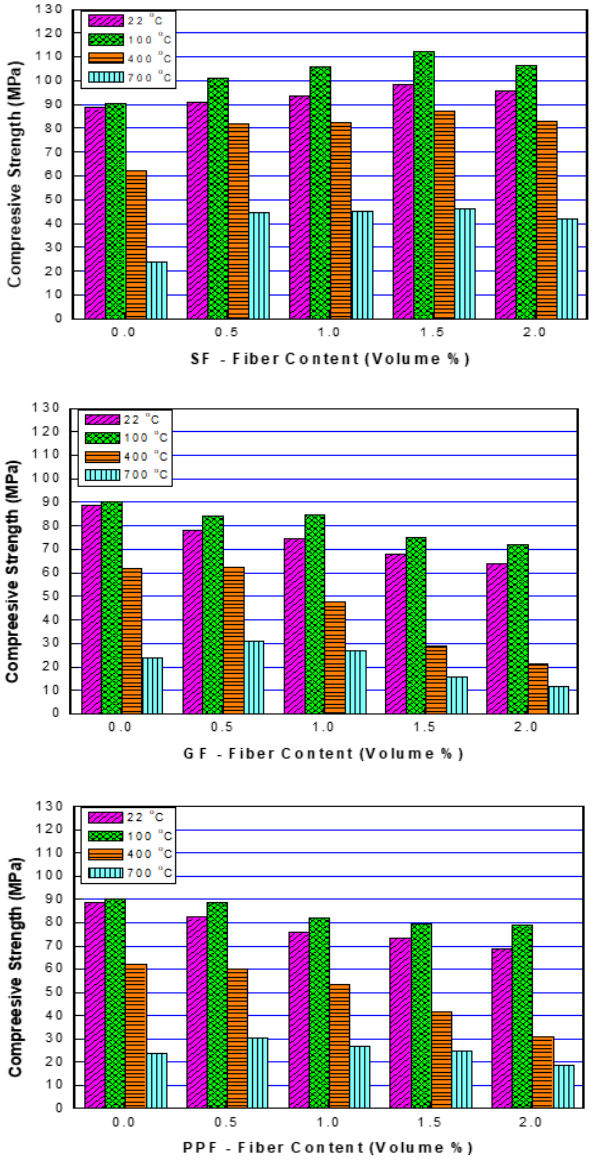

Fig. 4. Effect of fiber content on compressive strength at different temperatures (high strength concrete).

3.2. Flexural strength

The comparison between non-fibrous concrete and mixes incorporating with three distinctive fiber types subjected to four different temperatures. Fig. 5 and Table 4 show the flexural strength of NSC mixes under elevated temperature. When the temperature increases, the flexural strength of non-fibrous concrete reduces. The flexural strength of NSC without fibers reduces on average 67% at 400°C and about 82% at 700°C. The flexural strength of SF concrete mix reduces about 37% at 400°C (SF-2.0%) and on average 75% at 700°C (SF-2.0%). For GF, the reduction is about 53% at 400°C (GF-2.0%) and on average 90% at 700°C (GF-2.0%). According to PPF, the average decrease is 70% at 400°C (PPF-2.0%) and around 90% at 700°C (PPF-2.0%). Fig. 6 and Table 4 shows the flexural strength of HSC mixes under high temperature. It is observed that the flexural strength of non-fibrous concrete reduces when the temperature increases. The flexural strength of concrete without fibers reduces on average 72% at 400°C and about 88% at 700°C. The flexural strength of HSC with SF reduces about 40% at 400°C (SF-2.0%) and on average 76% at 700°C (SF-2.0%). While, GF mix, the reduction is on average 55% at 400°C (GF-2.0%) and about 90% at 700°C (GF-2.0%). And For PPF, the reduction is about 72% at 400°C (PPF-2.0%) and on average 90% at 700°C (PPF-2.0%).

Comparison between the results of the flexural strength for NSC and HCS (non-fibrous concrete and mixes incorporating with three different fiber types subjected to elevated temperatures from 22 to 700°C) are shown in Figs. 7 and 8. All types of fibers supply the concrete with the flexural strengths under high temperature. However, this supplying reduces while temperature increases. The decreasing of flexural strength of the concrete is due to the decomposition of calcium that depends on binding minerals of the concrete under elevated temperature (400°C and 700°C). The results are according to those in the studies of Çavdar (2012), Amin et al. (2020), and Mohammadhosseini et al. (2020).

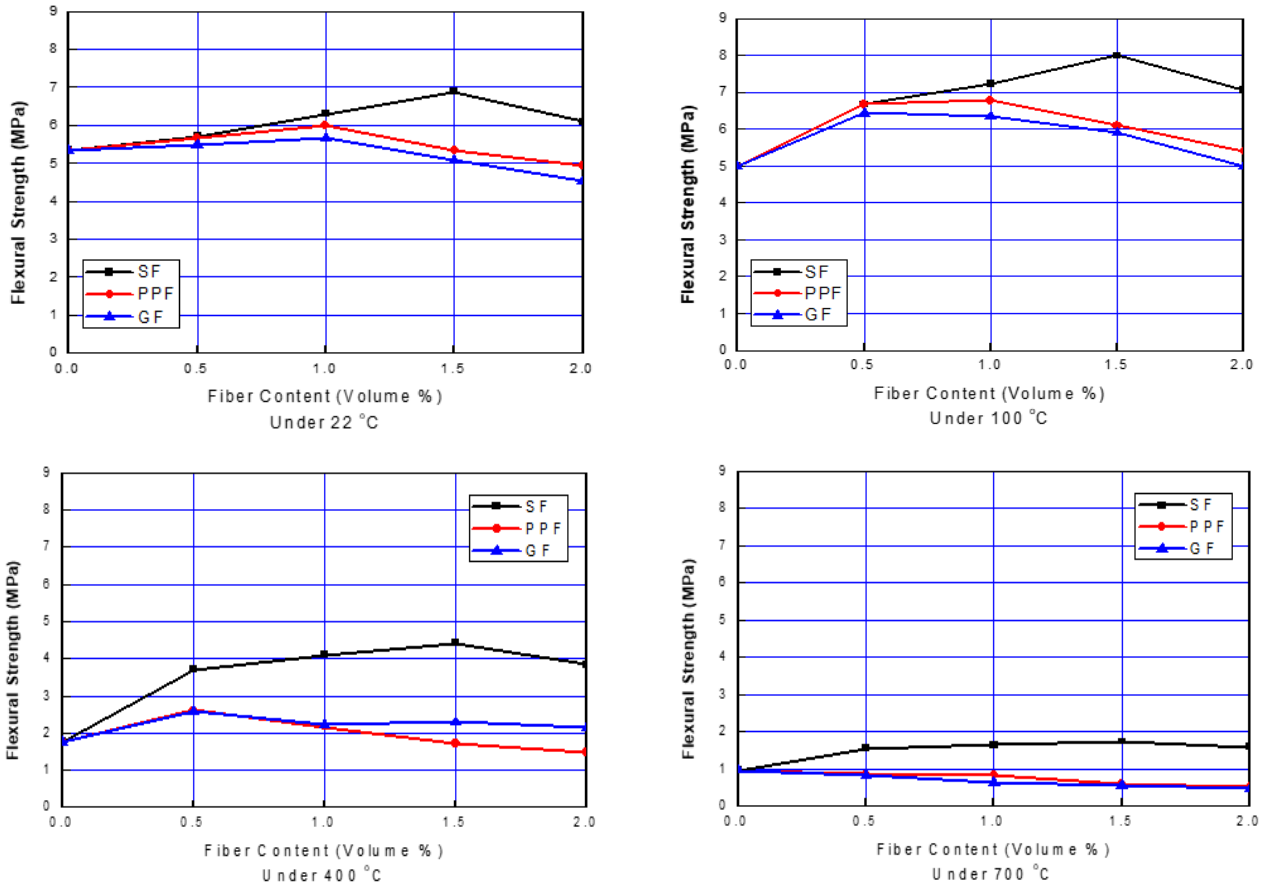

Fig. 5. Effect of fiber content on flexural strength at high temperature (normal strength concrete).

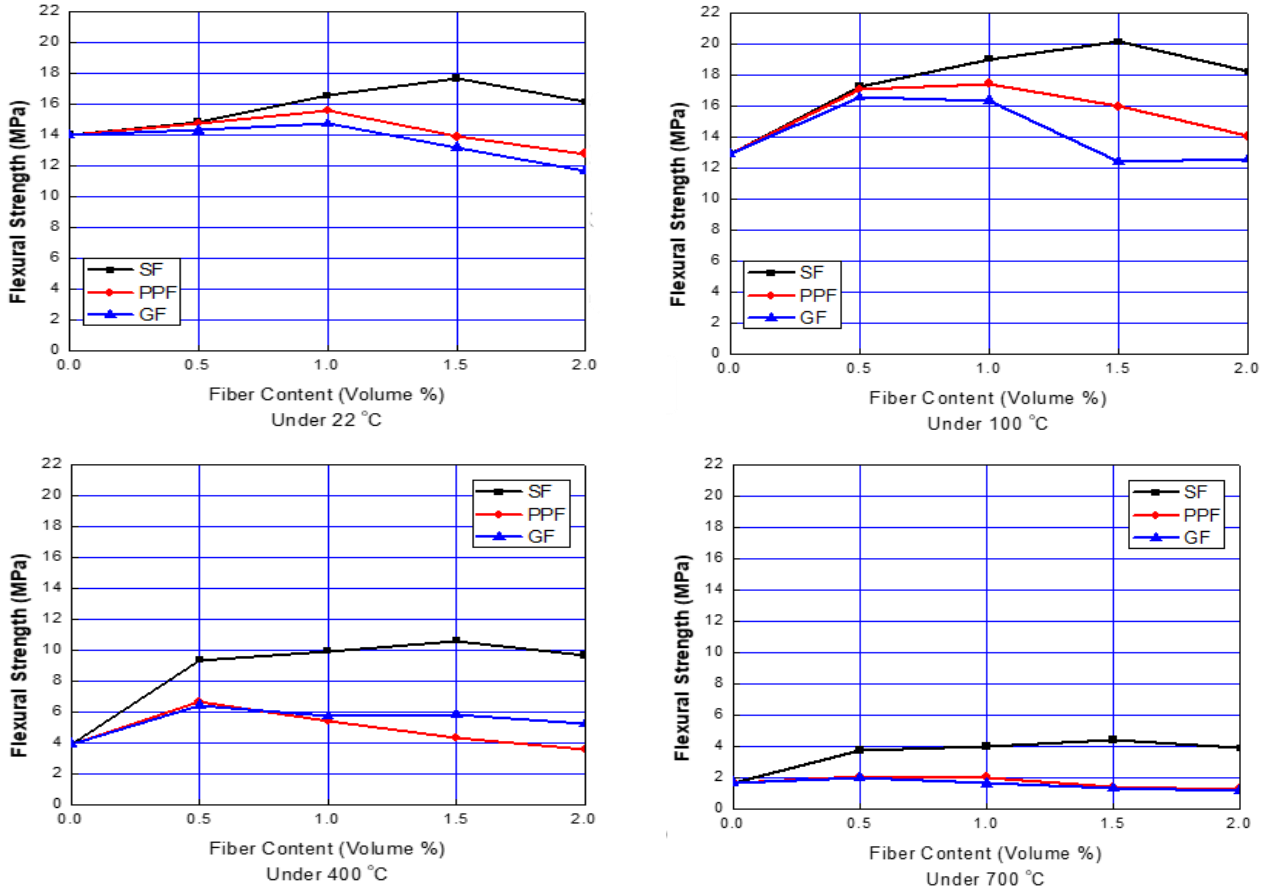

Fig. 6. Effect of fiber content on flexural strength at high temperature (high strength concrete).

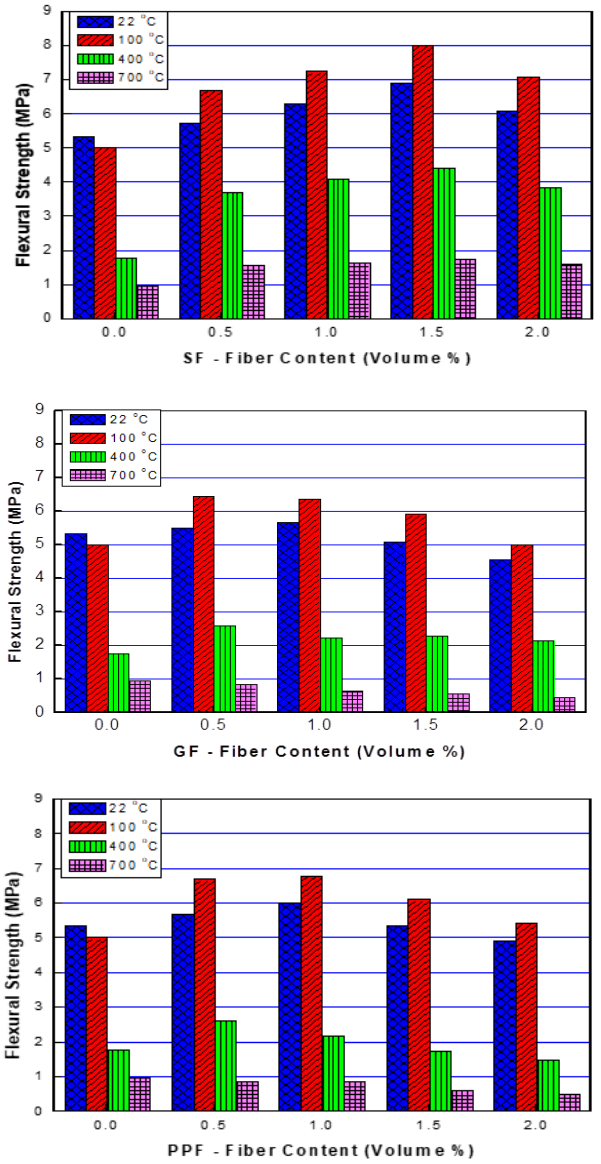

Fig. 7. Effect of fiber content on flexural strength at different temperatures (normal strength concrete).

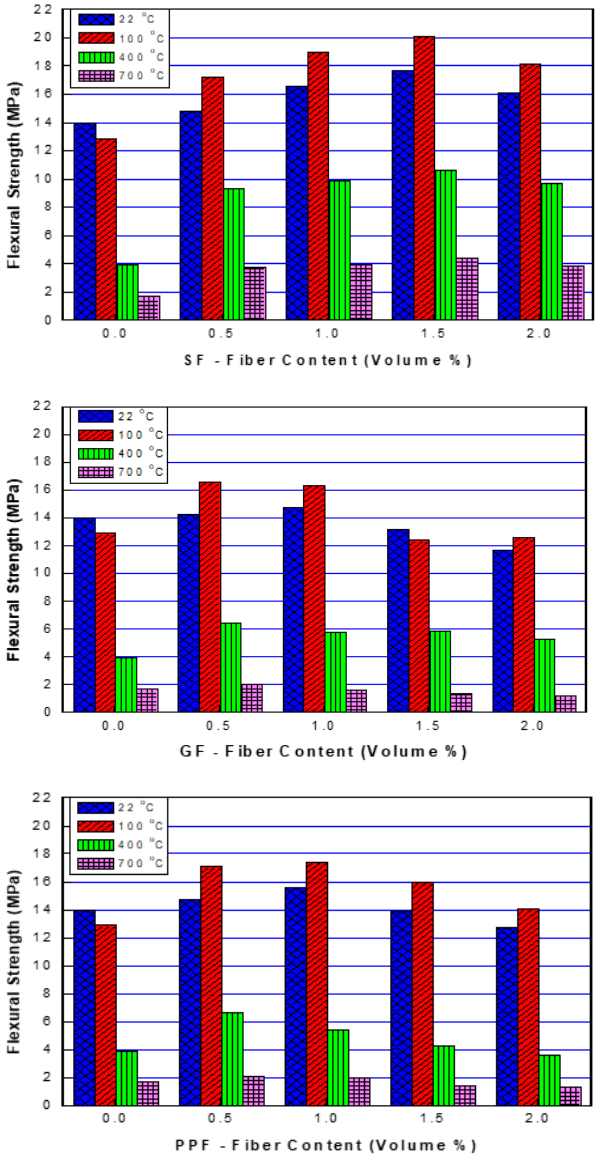

Fig. 8. Effect of fiber content on flexural strength at different temperatures (high strength concrete).

4. Conclusions

Based on the results found and reported, the following observations can be made:

- A slight reduction in the compressive strength and flexural strength of all mixtures was noted at the elevated temperature by adding used fibers. Despite the higher losses in the density of mixtures than those of control mix, the losses in compressive and flexural strengths values of mixes were considerably lower at elevated temperatures. However, beyond 400°C, the drop in strength values was more evident.
- With elevated in temperature, many changes happen in concrete of normal and high strength mixes. At 400°C, some cracks and deteriorations happen in matrices, while at 700°C, the cement matrices are weakened, and cracked.
- The compressive strength of non-fibrous normal strength concrete reduces about 10% at 400 °C and about 52% at 700°C. The compressive strength of the normal strength concrete with SF reduces about 10% at 400°C (SF-2.0%) and about 52% at 700°C (SF-2.0%). For GF, the reduction is about 63% at 400°C (GF-2.0%) and on average 80% at 700°C (GF-2.0%). And For PPF, the reduction is on average 52% at 400°C (PPF-2.0%) and about 70% at 700°C (PPF-2.0%).
- The compressive strength of HSC without fibers reduces on average 30% at 400°C and about 72% at 700°C. The compressive strength of HSC with SF reduces on average 13% at 400°C (SF-2.0%) and about 56% at 700°C (SF-2.0%). For GF, the reduction are about 67% at 400°C (GF-2.0%) and on average 82% at700°C (GF-2.0%). And For PPF, the reduction is on average 55% at 400 °C (PPF-2.0%) and about 73% at 700°C (PPF-2.0%).
- The flexural strength of NSC without fibers decreases about 67% at 400°C and about 82% at 700°C. The flexural strength of the normal strength concrete with SF reduces about 37% at 400°C (SF-2.0%) and

about 75% at 700°C (SF-2.0%). For GF, the reduction is on average 53% at 400°C (GF-2.0%) and about 90% at 700°C (GF-2.0%). And For PPF, the reduction is about 70% at 400°C (PPF-2.0%) and on average 90% at 700°C (PPF-2.0%).

- The flexural strength of high strength concrete without fibers reduces about 72% at 400°C and about 88% at 700°C. The flexural strength of the high strength concrete with SF reduces on average 40% at 400°C (SF-2.0%) and about 76% at 700°C (SF-2.0%). For GF, the reduction is on average 55% at 400°C (GF-2.0%) and about 90% at700 °C (GF-2.0%). And for PPF, the reduction is on average 72% at 400°C (PPF-2.0%) and about 90% at 700°C (PPF-2.0%).
- The flexural strengths and compressive strengths for NSC and HSC mixes at 28 days under high temperature decreases as the temperature increases especially up to 400°C.
- Each fiber shows the best performance at different addition ratios when flexural and compressive strength are taken into consideration along with temperature. The highest increase in flexural strength and lowest decrease in compressive strength is at 0.5–1.5% fiber addition ratio for PPF and GF if all temperature conditions are taken into consideration. And for SF, it is 1.5% by volume.

Acknowledgements

Authors would like to thank Delta University for Science and Technology and Suez University for the support provided for this research.

References

Altun MG, Oltulu M (2020). Effect of different types of fiber utilization on mechanical properties of recycled aggregate concrete containing silica fume. *Journal of Green Building*, 15(1), 119–136.

Amin M, Tayeh BA, Agwa IS (2020). Investigating the mechanical and microstructure properties of fibre-reinforced lightweight concrete under elevated temperatures. *Case Studies in Construction Materials*, 13, e00459.

Anderberg Y (1997). Spalling phenomena of HPC and OC. *International Workshop on Fire Performance of High-Strength Concrete*, NIST, 69–73.

Bažant ZP, Kaplan MF (1996). Concrete at High Temperatures: Material Properties and Mathematical Models. Longman.

Çavdar A (2012). A study on the effects of high temperature on mechanical properties of fiber reinforced cementitious composites. *Composites Part B: Engineering*, 43(05), 2452–2463.

Cree D, Pliya P, Green MF, Noumowé A (2017). Thermal behaviour of unstressed and stressed high strength concrete containing polypropylene fibers at elevated temperature. *Journal of Structural Fire Engineering*, 8(4), 402–417.

Cülfik MS, Özturan T (2010). Mechanical properties of normal and high strength concretes subjected to high temperatures and using image analysis to detect bond deteriorations. *Construction and Building Materials*, 24(08), 1486–1493.

Daniel JI, Ahmad SH, Arockiasamy M, Ball HP et al. (2002). State-of-the-art report on fiber reinforced concrete reported by ACI Committee 544. In ACI.544.1R-96, American Concrete Institute, USA.

Georgali B, Tsakiridis PE (2005). Microstructure of fire-damaged concrete. A case study. *Cement and Concrete Composites*, 27(02), 255–259.

Ghugal YM, Deshmukh SB (2006). Performance of alkali-resistant glass fiber reinforced concrete. *Journal of Reinforced Plastics and Composites*, 25(6), 617–630.

Hilles MM, Ziara MM (2019). Mechanical behavior of high strength concrete reinforced with glass fiber. *Engineering Science and Technology, an International Journal*, 22(3), 920–928.

Juan-García P, Torrents JM, López-Carreño RD, Cavalaro SHP (2016). Influence of fiber properties on the inductive method for the steel-fiber-reinforced concrete characterization. *IEEE Transactions on Instrumentation and Measurement*, 65(8), 1937–1944

Kuder KG, Shah SP (2010). Processing of high-performance fiber-reinforced cement-based composites. *Construction and Building Materials*, 24(02), 181–186.

Mohammadhosseini H, Alrshoudi F, Md Tahir M, Alyousef R, Alghamdi H, Alharbi YR, Alsaif A (2020). Performance evaluation of novel prepacked aggregate concrete reinforced with waste polypropylene fibers at elevated temperatures. *Construction and Building Materials*, 259, 120418.

Noumowe AN, Siddique R, Debicki G (2009). Permeability of high-performance concrete subjected to elevated temperature (600°C). Construction and Building Materials, 23(5), 1855–1861.

Pavlík J, Poděbradská J, Toman J, Černý R (2002). Thermal properties of carbon- and glass fiber reinforced cement composites in high temperature range in a comparison with mortar and concrete. *Thermophysics*, 47–52.

Peled A, Jones J, Shah SP (2005). Effect of matrix modification on durability of glass fiber reinforced cement composites. *Materials and Structures/Materiaux et Constructions*, 38(276), 163–171.

Purnell P, Short NR, Page CL, Majumdar AJ (2000). Microstructural observations in new matrix glass fibre reinforced cement. *Cement and Concrete Research*, 30(11), 1747–1753.

Raza SS, Qureshi LA, Ali B, Raza A, Khan MM, Salahuddin H (2020). Mechanical properties of hybrid steel–glass fiber-reinforced reactive powder concrete after exposure to elevated temperatures. *Arabian Journal for Science and Engineering*, 45(5), 4285–4300.

Şahmaran M, Özbay E, Yücel HE, Lachemi M, Li VC (2011). Effect of fly ash and PVA fiber on microstructural damage and residual properties of engineered cementitious composites exposed to high temperatures. *Journal of Materials in Civil Engineering*, 23(12), 1735–1745.

Sanjayan G, Stocks LJ (1993). Spalling of high-strength silica fume concrete in fire. *ACI Materials Journal*, 90(2), 170–173.

Tanyildizi H (2008). Effect of temperature, carbon fibers, and silica fume on the mechanical properties of lightweight concretes. *Xinxing Tan Cailiao/ New Carbon Materials*, 23(4), 339–344.

Zheng D, Song W, Fu J, Xue G, Li J, Cao S (2020). Research on mechanical characteristics, fractal dimension and internal structure of fiber reinforced concrete under uniaxial compression. *Construction and Building Materials*, 258, 120351.

Zhong C, Liu M, Zhang Y, Wang J, Liang D, Chang L (2020). Study on mechanical properties of hybrid polypropylene-steel fiber RPC and computational method of fiber content. *Materials*, 13(10), 1–21.